Supporting Information

Biobased Polyurethane foams based on new polyols architectures from microalgae oil

Julien Peyrton† , Clémence Chambaretaud†,‡, Alexandru Sarbu‡, and Luc Avérous†,*

† BioTeam/ICPEES-ECPM, UMR CNRS 7515, Université de Strasbourg, 25 rue Becquerel, 67087 Strasbourg, Cedex 2, France

‡ Soprema, 14 rue de Saint-Nazaire, 67025 Strasbourg, Cedex 1, France

* Corresponding Author email: luc.averous@unistra.fr

Number of Pages: 38

Number of Tables: 6

Number of Figures: 29

Number of Schemes: 2

Polyols analysis procedures

The ^{1}H NMR analyses were realized on a 400 MHz Bruker spectrometer. Deuterated chloroform ($CDCl_3$) was used as solvent to prepare the samples. The ^{1}H NMR number of scans was set to 32. Each spectrum was calibrated with the $CDCl_3$ signal, being set at δ=7.26 ppm.

Iodine value (IV) is the measure of the double bond content expressed in grams of iodine (I_2) per hundred grams of sample. It was determined using the Wijs method. Approximately 200 mg of precisely weighed sample was diluted in 10 mL of cyclohexane:acetic acid (1:1) solution. Then, 20 mL of Wijs solution composed of 1.0 M of iodine chloride in acetic acid was added. The solution was left in a dark place for one hour. 20 mL of potassium iodide solution in water and 100 mL of water were added to quench the excess of potassium iodide. The solution was then rapidly titrated with a 0.1 mol/L solution of sodium thiosulfate ($Na_2S_2O_3$). Starch was used as an indicator. IV is determined according to Equation S1.

$$IV = \frac{(V_{Bl} - V_{eq}) * C_{TS} * 126.9}{W_S} * 100 \qquad (S1)$$

Where V_{Bl} is the blank equivalence volume, V_{eq} the equivalence volume, C_{TS} the concentration of the thiosulfate solution, 126.9 half of the molar mass of iodine molecule and W_s the sample weight.

EI is expressed in wt% of oxygen in the form of epoxides in the fatty compound. In an Erlenmeyer flask, between 150 and 200 mg of sample was precisely weighed and dissolved in 5 mL of MEK. Exactly 10 mL of 0.4 mol/L HCl solution in MEK was added. The flask was closed and left to react at ambient temperature under magnetic stirring for 30 min. Then 3 mL of water was added. The excess of HCl is titrated with 0.1 mol/L KOH solution. Phenolphthalein was used as the equivalence indicator. The epoxide index is determined according to Equation S2.

$$EI = \frac{(V_{Bl} - V_{eq} + V_{Ac}) * C_{KOH}}{W_S * 10} * 16 \qquad (S2)$$

Where V_{Bl} is the blank equivalence volume, V_{eq} the equivalence volume, V_{Ac} the volume of acid titration (without adding HCl solution), C_{KOH} the concentration of the KOH solution, 16 is the molar mass of oxygen and W_s the sample weight.

I_A is expressed in milligrams of KOH required to neutralize all acid moieties in one gram of oil. Between 1 and 3 grams of sample was weighed in a beaker and dissolved with a 1:1 solution of ethanol:diethyl ether. The solution is directly titrated with a 0.1 mol/L KOH solution. Phenolphthalein is used as the equivalence indicator. The I_A is calculated according to Equation S3.

$$I_A = \frac{V_{eq} * C_{KOH} * 56.1}{W_S} \qquad (S3)$$

Where V_{eq} the equivalence volume, C_{KOH} the concentration of the KOH solution, 56.1 the molar mass of KOH and W_s the sample weight.

I_{OH} is a key parameter in polyol characterization. It is expressed in milligrams of KOH equivalent to OH content in one gram of polyol. I_{OH} can be determined by ^{31}P NMR-assisted titration method.[1] According to a previously described protocol,[2] approximately 20 mg of precisely weighed sample precisely weighted was diluted in 500 µl of 1:1.6 $CDCl_3$/pyridine mixture, 100 µl of 0.01 mol/L cholesterol solution (internal standard) and 100 µl of chromium acetylacetonate [$Cr(acac)_3$; 5 mg/mL] (relaxation agent) was added. After thorough mixing, 100 µl of 2-chloro-4,4,5,5-tetramethyl-1,3,2-dioxapholane (phospholane reagent) was added to the solution. The sample was stirred at room temperature for one hour and then transferred into an NMR-tube. ^{31}P NMR analyses were performed with the use of a Bruker 400 MHz spectrophotometer, and the number of scans was set to 128 at 25 °C. Peak analysis and quantitative analysis were performed according to previous reports.[3]

Rheological measurements were carried out on a TA instrument discovery HR-3 using parallel plate geometry. The viscosity was measured with a shear rate varying from 10^{-5} to 100 s^{-1} in 5 min, and after 10 min of rest, the shear rate varied from 100 to 10^{-5} s^{-1} in 5 min. The viscosity values were taken at the plateau region for different temperatures.

The polyols functionality was determined based on the Flory-Stockmayer[4-5] equation applied to a reaction between a polyisocyanate and a polyol, described in Equation S4.

$$r * p_{NCO} = \frac{1}{(f_{OH} - 1)(f_{NCO} - 1)} \tag{S4}$$

This equation mathematically explains the relation at the gel point between the molar ratio of OH over NCO (r), the isocyanate conversion at the gel point (p_{NCO}) and the average functionality of the monomers (f_{OH} and f_{NCO}). The equation relies on three hypotheses (i) all functions are equally reactive, (ii) there is no intramolecular reaction and (iii) the network is only formed by the reaction between the polyol and the isocyanate. The hydroxyl is in excess so that the conversion of isocyanate is complete. Moreover, the use of a diisocyanate transformed Equation S4 to Equation S5.

$$r = \frac{1}{(f_{OH} - 1)} \tag{S5}$$

A series of materials with different r ratios were produced. The full conversion of isocyanate was controlled by FTIR and the disappearance of the band associate to isocyanate at $\tilde{v}$=2260-2240 cm^{-1}. The rheological behavior at the gel point was described by Winter & Chambon.[5,6] The rheological experiments were performed on a TA Instrument Discovery HR-3 using parallel 20 mm geometry. The samples were analyzed in oscillatory conditions, applying a strain of 0.1 % between 0.01 and 80 Hz. The linear viscoelastic domain conditions were determined before the functionality determination by applying a strain from 0.001 % to 5 % at a frequency of 80 Hz on a sample with equimolar component (r = 1). For r = 1, one should obtain the most cross-linked material, which translates into the most brittle sample.

The size exclusion chromatography experiments were performed with an Acquity-APC (Waters) in tetrahydrofuran (THF) equipped with three columns (Acquity APC XT 450 Å 2.5µm 4.6 x 150 mm, 200 and 45) heated at 40 °C. Before the injection, samples were dissolved in THF and filtered with a 0.2 µm PTFE membrane. Polystyrene standard samples were used for the molar mass calibration.

ATR FTIR spectra were recorded on Thermo Scientific Nicolet iS210 instrument using a Smart Orbit Diamond. An atmospheric background was collected before each sample analysis (32 scans, resolution 4 cm^{-1}).

TGA was performed using a TA Instrument Hi-Res TGA Q5000 under N_2 (flow rate 25 mL/min). Samples of 1–3 mg were heated from room temperature to 700 °C at 10 °C/min. The main characteristic degradation temperatures were determined at the maximum of the DTG curve.

Foam analysis

The main foam characteristic times are the cream time (the beginning of the foam rising initiated by the water-isocyanate reaction), the gel time (linked to the formation of the thermoset network) and the tack-free time (time to cure the surface), which were recorded for each foam. Core temperature, foam height and expansion rate were recorded using a Foamat FPM 150 (Messtechnik GmbH, Germany). The apparatus was equipped with a cylindrical container (180 mm in height and 75 mm in radius), an ultrasonic probe (recording with ultrasound waves the foam height), a Pt sensor (for the temperature). The data were recorded and analyzed using dedicated software.

Closed-cell content was determined using an Ultrapyc 1200e from Quantachrome instruments based on the technique of gas expansion (Boyle's law). Cubic foam samples (roughly 2.5 cm × 2.5 cm × 2.5 cm) were cut for the first measurement, then the sample was sectioned once more into eight pieces, and measurement was re-run to correct the closed-cell content based on closed cells which were cut open during slicing. Measurements were performed according to EN ISO4590 and ASTM 6226 techniques.

Parallelepipedic foam samples were measured with a caliper and weighed to determine the apparent foam density.

Foam cell morphology was observed with a Vega-3 (Tescan) emission scanning electron microscope. Cubic foam samples were cut with a microtome blade and were analyzed in two characteristic orientations: parallel and perpendicular to the foam rise direction denoted

as longitudinal and transversal direction, respectively. Before the examination, samples were coated with a thin layer of gold using a sputter coater (Quorum Q 150 RS, Quo-rum Technologies). Using ImageJ software (Open source program), the cell average size was measured as well as the cell anisotropy coefficient defined by Equation S6.[8]

$$R = \frac{1}{n} \sum_{i=1}^{n} \frac{D_{iF}^{\max}}{D_{iF}^{\min}} \qquad (S6)$$

Where $D_F^{\max}$ and $D_F^{\min}$ are the maximum and minimum cell Feret diameters and n is the number of measured cells for a given sample. The number of measured cells is ranging from 200 to 1500 in both directions.

The quasi-static compression tests were carried out with an Instron 3367 compression testing machine, equipped with a 30 kN load sensor, at room temperature and constant strain rate of 6 mm/min. The sample size for the compression test was 100 mm x 100 mm x 60 mm. Samples were compressed in the longitudinal direction (corresponding to the foam rise) until 10 % of deformation is reached. The test was realized according to the EN 826 standard method, and the data were recorded and analyzed using the Bluehill 3 software.

Thermal conductivity measurements were carried out with a Heat flowmeter HFM 436 from Netzsch. The measurements were performed according to the EN 12667 standard procedure. Typically, the setup consists of a hot and a cold plate equipped with two thermocouples to determine their temperatures. The device is also equipped with sensors dedicated to the measurement of the heating time and the cycle time. The heat and cycle times were used to correct the maximum conduction heat flux, which is necessary for the determination of the thermal conductivity coefficient, through the Fourier law, assuming steady-state thermal condition. Specimens of different foams, with dimensions of 175 mm × 175 mm × 60 mm, have been used for the determination of the thermal conductivity coefficient. The data were recorded and analyzed using QLab software.

Characterization of MAO

Table S1. Fatty acid profile of MAO.

Fatty acids	C14:0	C16:0	C16:1	C18:0	C18:1	C18:3	C18:4	C20:3	C20:5	C22:0	C22:5	C22:6	Other
Distribution(%)	1.5	21.8	0.2	0.9	0.3	0.3	0.1	1.0	0.5	0.6	9.9	60.2	2.7

The triglyceride structure is identified by glyceryl protons (i) and (h) at δ=5.3 ppm and 4.1-4.4 ppm, respectively. The signal at δ=0.88 ppm (a) is characteristic of the terminal methyl groups of fatty acids. When a double bond is located at the third carbon from the terminal methyl group (omega-3 acid), this group signal appeared downfield at δ=0.97 ppm (a'). The methylene protons (b) were located between δ=1.2 and 1.4 ppm. Signals of protons in the vicinity of the carbonyl groups (c) and (e) were observed at δ=1.6 and 2.3 ppm, respectively. In the case of C22:6 or C22:5 the vicinity of the double bond shifts those signals downfield at δ= 2.4 ppm (f). Allyls protons positioned between two double bonds (g) were located at δ=2.8 ppm. The vinyl protons, (j) were located at δ=5.4 ppm. According to NMR calculation, the average double bond functionality of MAO is 12.
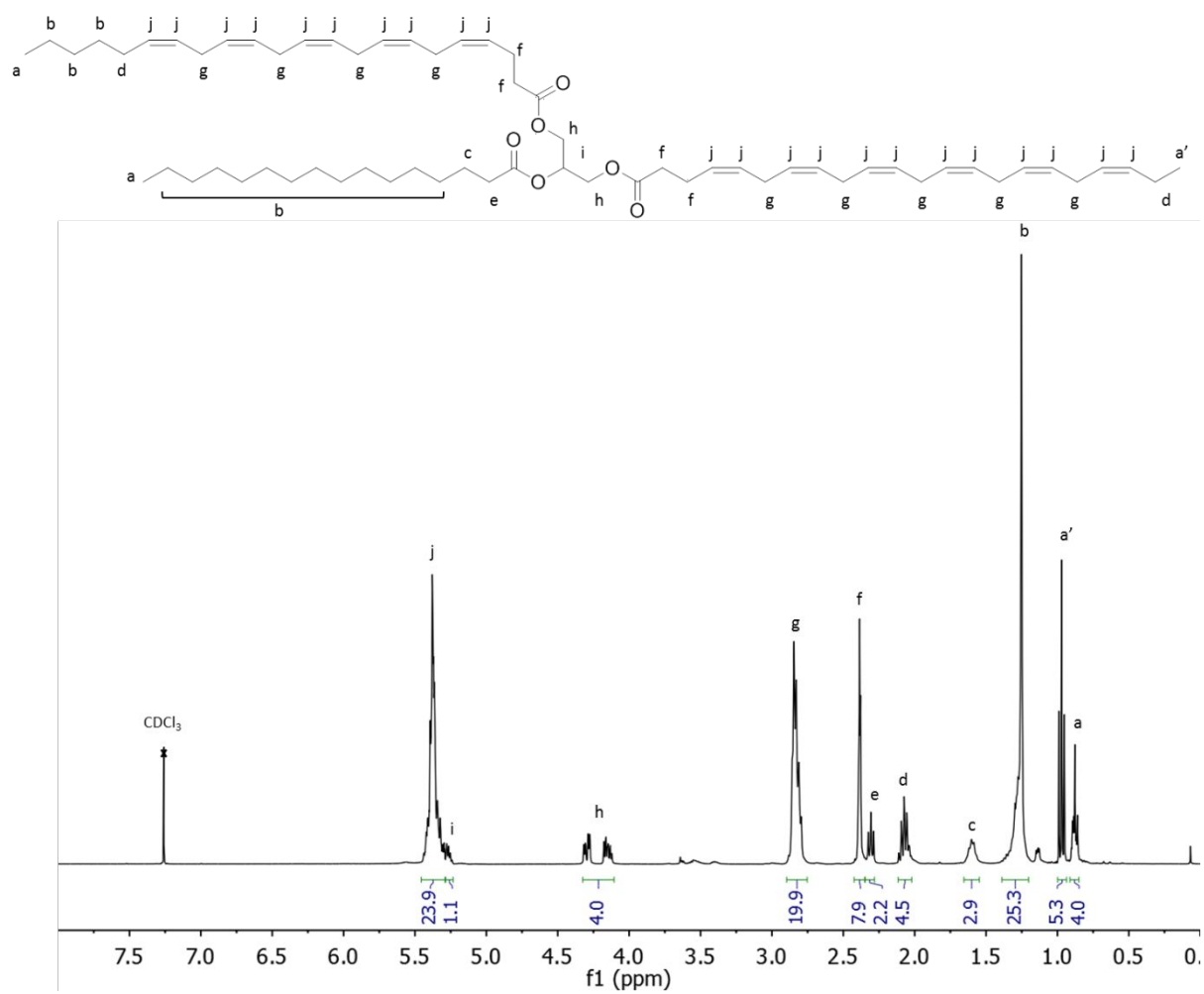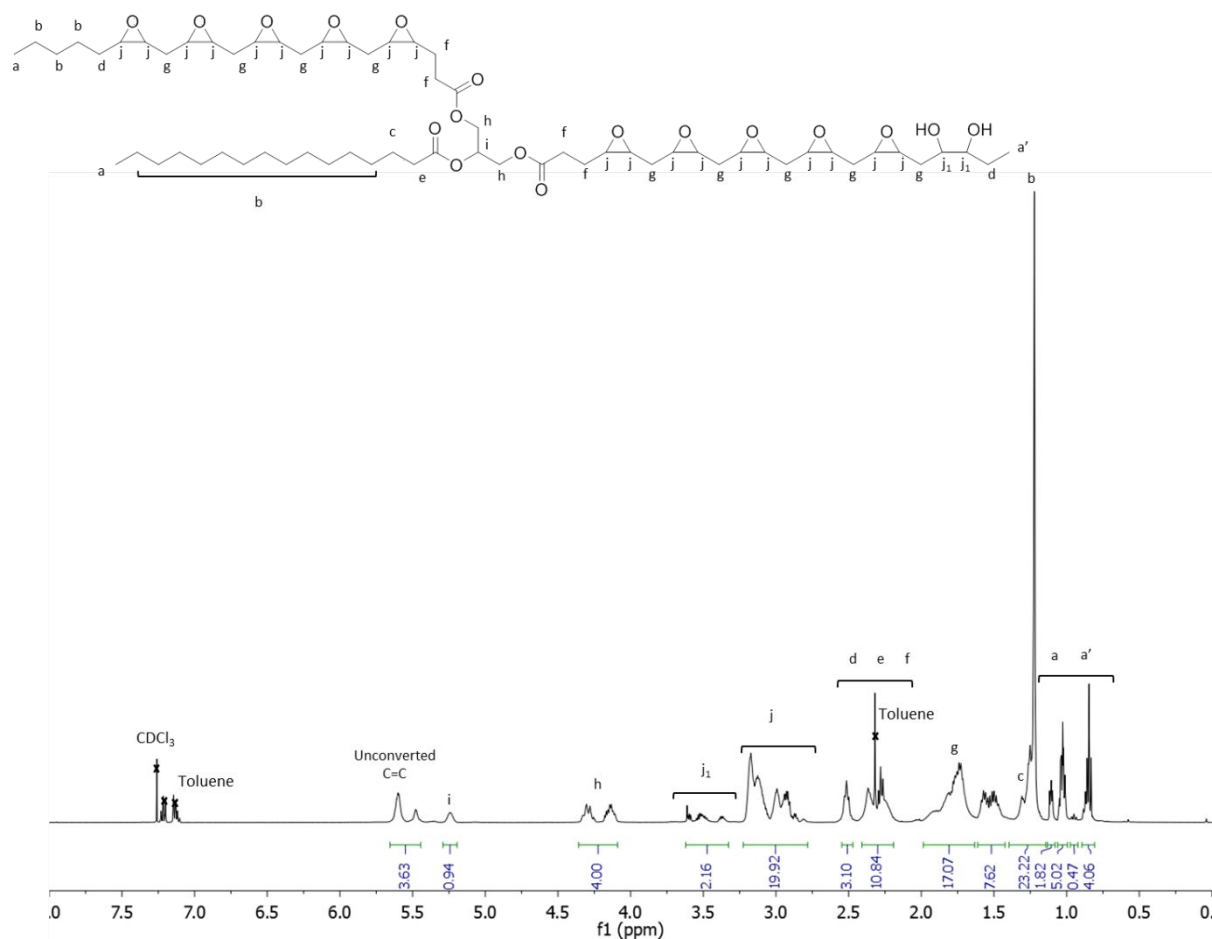
Figure S1. Proton NMR spectrum of MAO.

EMAO synthesis

Protocol of MAO epoxidation

According to a previously described protocol[9], 11,1 kg of MAO (145 mol, 1eq), 6 L toluene and 2.2 kg of formic acid (48 mol, 0.33 eq) were introduced in a 100 L reactor equipped with a reflux condenser, a mechanical stirrer and a dropping funnel. The mixture was heated at 40 °C under an inert atmosphere with a 250 rpm agitation for one hour. Then, 31.2 kg of H_2O_2 (35 %) (360 mol, 2.45 eq) was added slowly over 5h not to raise the temperature above 75 °C under the agitation of 500 rpm. The mixture turned white and thickened along with the reaction. Once the addition finished, the temperature is stabilized between 70 °C and 75 °C and the mixture is stirred for 3 hours. The viscosity of the mixture was decreased by 5 L of toluene. The organic phase was washed with 20 L of water at 65 °C until neutral pH. The solvent was evaporated under reduced pressure. 9.89 kg of epoxidized MAO (EMAO) was obtained with 74 wt% and 80 mol% yield.
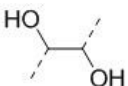
^1H NMR (400 MHz, $CDCl_3$): δ =5.63-5.45 (m, 1H; C=C)), 5.25 (tt, 1H; CH-Glycerine), 4.30 (d, 2H; CH_2-Glycerine), 4.15 (d, 2H; CH_2-Glycerine), 3.2-2.8 (m, 2H; epoxide), 1.35–1.13 (m, 30H; aliphatic CH_2), 1.03 (t,3H; CH_3-CH_2-Epoxide), 0.88 ppm (t, 3H; CH_3).

IR: ṽ = 3500 (OH vibration), 1738 (Ester, C=O Stretching), 826 cm^{-1} (epoxide vibration)

Figure S2. Proton NMR spectrum of EMAO.

Table S2. Repartition of the different chemical moieties in the EMAO.

Name	Structure	Molar quantity (%)
Double bond		16 %
Epoxide		80 %
Hydroxyl		4 %

Polyol synthesis

Ring-opening of EMAO with acetic acid (EMAO-AA)

The protocol was adapted from a previously published work.[10] The reaction was carried out in a round bottom flask equipped with a reflux condenser and a mechanical stirrer. The flask was filled with 500 g of MAO 11 mmol epoxide/g (5.5 mol, 1 eq) and 1.6 L of acetic acid (28 mol, 5 eq). The mixture was stirred at 90 °C for 24 hours. 500 mL of ethyl acetate were added to decrease the viscosity of the mixture. The organic phase was washed with saturated $NaHCO_3$ solution until neutral pH. Then it was washed with brine solution, dried with anhydrous sodium sulfate and then filtered. The solvent was evaporated under reduced pressure. The ring-opened EMAO with acetic acid (EMAO-AA) was dried overnight in a vacuum oven at 40 °C. The yield was 73 wt%.

^{1}H NMR (400 MHz, $CDCl_3$): δ=5.63-5.45 (m, 1H; C=C)), 5.25 (tt, 1H; CH-Glycerine), 1.35–1.13 (m, 30H; aliphatic CH_2), 0.88 ppm (t, 3H; CH_3).

FTIR: ṽ = 3500 (OH vibration), 1734 cm^{-1} (Ester, C=O Stretching)

Ring-opening of EMAO with Ethanol (EMAO-EtOH)

The protocol was adapted from a previously published work.[10,11] The reaction was carried out in a round bottom flask equipped with a reflux condenser and a mechanical stirrer. The flask was filled with 500 g of MAO 11 mmol epoxide/g, (5.5 mol, 1 eq), 50 g of Amberlyst® 15H and 1.5 L of ethanol (25.7 mol, 4.7 eq). The mixture was stirred at 90 °C for 24 hours. The catalyst was removed by filtration. 500 mL of ethyl acetate were added to decrease the viscosity of the mixture. Then the organic phase was treated with $NaHCO_3$ and water until the pH was neutral. Then it was washed with brine solution, dried with anhydrous sodium sulfate and then filtered. The solvent was evaporated under reduced pressure. The ring-opened EMAO with ethanol (EMAO-EtOH) was dried overnight in a vacuum oven at 40 °C. The yield was 76 wt%.

^{1}H NMR (400 MHz, $CDCl_3$): δ=5.63-5.45 (m, 1H; C=C)), 5.25 (tt, 1H; CH-Glycerine), 1.35–1.13 (m, 30H; aliphatic CH_2), 0.88 ppm (t, 3H; CH_3).

FTIR: ṽ = 3500 (OH vibration), 1733 cm^{-1} (Ester, C=O Stretching)

Ring-opening of EMAO with diethylamine (EMAO-DEA)

The protocol was adapted from a previously published work.[10,12] The reaction was carried out in a round bottom flask equipped with a reflux condenser and a mechanical stirrer. The flask was filled with 500 g of MAO 11 mmol epoxide/g (5.5 mol, 1 eq), 180 g of $ZnCl_2$ (1.3 mol, 0.24 eq) and 0.9 L of diethylamine (8.7 mol, 1.6 eq). The mixture was stirred at 110 °C for 24 hours. The catalyst was removed by filtration. 500 mL of ethyl acetate were added to decrease the viscosity of the mixture. Then the organic phase was treated with $NaHCO_3$ and water until the pH was neutral. Then it was washed with brine solution, dried with anhydrous sodium sulfate and then filtered. The solvent was evaporated under reduced pressure. The ring-opened EMAO with diethylamine (EMAO-DEA) was dried overnight in a vacuum oven at 40 °C. The yield was 78 wt%.

^{1}H NMR (400 MHz, CDCl$_3$): δ=5.63-5.45 (m, 1H; C=C)), 5.25 (tt, 1H; CH-Glycerine), 1.35–1.13 (m, 30H; aliphatic CH$_2$), 0.88 ppm (t, 3H; CH$_3$).

FTIR: ṽ = 3500 (OH vibration), 1732 cm^{-1} (Ester, C=O Stretching)

Ring-opening of EMAO with hydrochloric acid (EMAO-HCl)

The protocol was adapted from a previously published work.[10,13] The reaction was carried out in a round bottom flask equipped with a reflux condenser and a mechanical stirrer. The flask was filled with 500 g of MAO 11 mmol epoxide/g (5.5 mol, 1 eq), 500 mL of HCl (6 mol, 1.1 eq) and 0.6 L of acetone. To avoid overheating, the hydrochloric acid (1.5 eq) was added dropwise in a water-ice bath. The mixture was stirred at room temperature for 2 hours. At the end, the mixture was recovered in 300 mL of ethyl acetate and deionized water. The organic phase was treated with $NaHCO_3$ until neutral pH. Then it was washed with brine solution, dried over anhydrous sodium sulfate and then filtered. The solvent was evaporated under reduced pressure. The ring-opened EMAO with hydrochloric acid (EMAO-HCl) was dried overnight in a vacuum oven at 40 °C. The yield was 86 wt%.
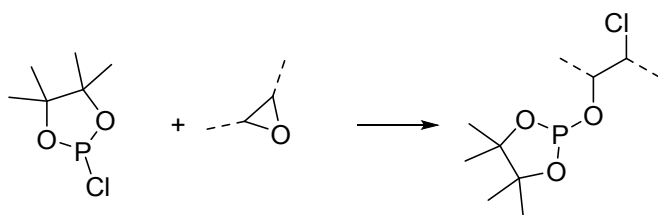
^{1}H NMR (400 MHz, CDCl$_3$): δ=5.63-5.45 (m, 1H; C=C)), 5.25 (tt, 1H; CH-Glycerine), 1.35–1.13 (m, 30H; aliphatic CH$_2$), 0.88 ppm (t, 3H; CH$_3$).

FTIR: ṽ = 3500 (OH vibration), 1732 cm^{-1} (Ester, C=O Stretching)
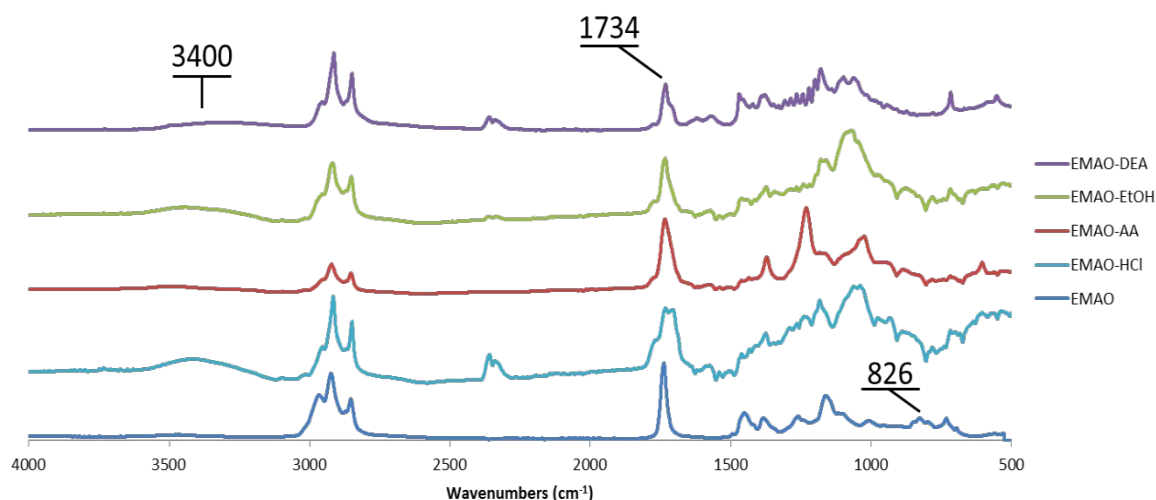
^{31}P I$_{OH}$ measurements
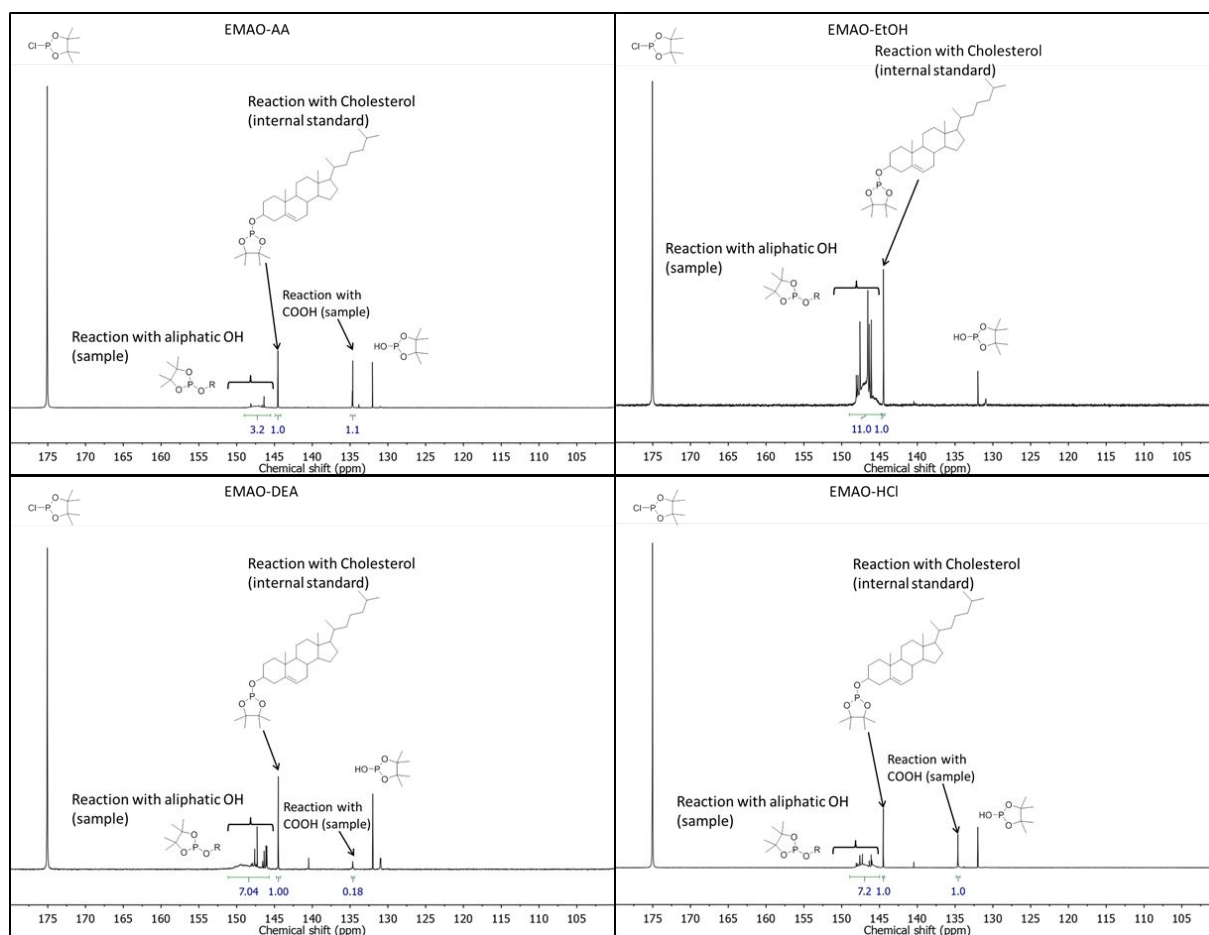
Figure S3. ^{31}P NMR analysis for hydroxyl titration of EMAO-AA, EMAO-EtOH, EMAO-DEA and EMAO-HCl.

**Scheme S1.** Possible reaction of epoxide ring-opening by phospholane reagent.

Structural characterizations of polyols

Figure S4. FTIR spectra of EMAO, EMAO-HCl, EMAO-AA, EMAO-EtOH and EMAO-DEA.

For all the polyols synthesized, the conversion of epoxide to hydroxyl groups should be expected to be higher. However, during ring-opening reactions, side reactions can occur, as presented in Scheme S2. First of all, under acidic conditions[14] or with a coordination agent,[15] hydroxyl groups already formed can protonate and attack an epoxide on another molecule, leading to homopolymerization (Scheme S2-**A**). Under milder acidic conditions, only oligomers were formed. Wang *et al.* demonstrated ether oligomers formation by ring-opening of a fatty epoxide by carboxylic acid.[16] Furthermore, the proximity of the epoxide on the EMAO molecules could lead to an intramolecular attack (Scheme S2-**B**). Depending on the ring-opening position and attack of the hydroxyl, 4, 5 or 6 membered cyclic ethers could be formed. The low-intensity peaks detected between δ=3.2 and 4.0 ppm in the ^{1}H NMR spectra, presented in Figure S5 and S6 in SI, are in the typical range of ether signals. Theses NMR peaks could be indicatives of the epoxide polymerization side reactions and thus accounts as to why such low I_{OH} were observed.
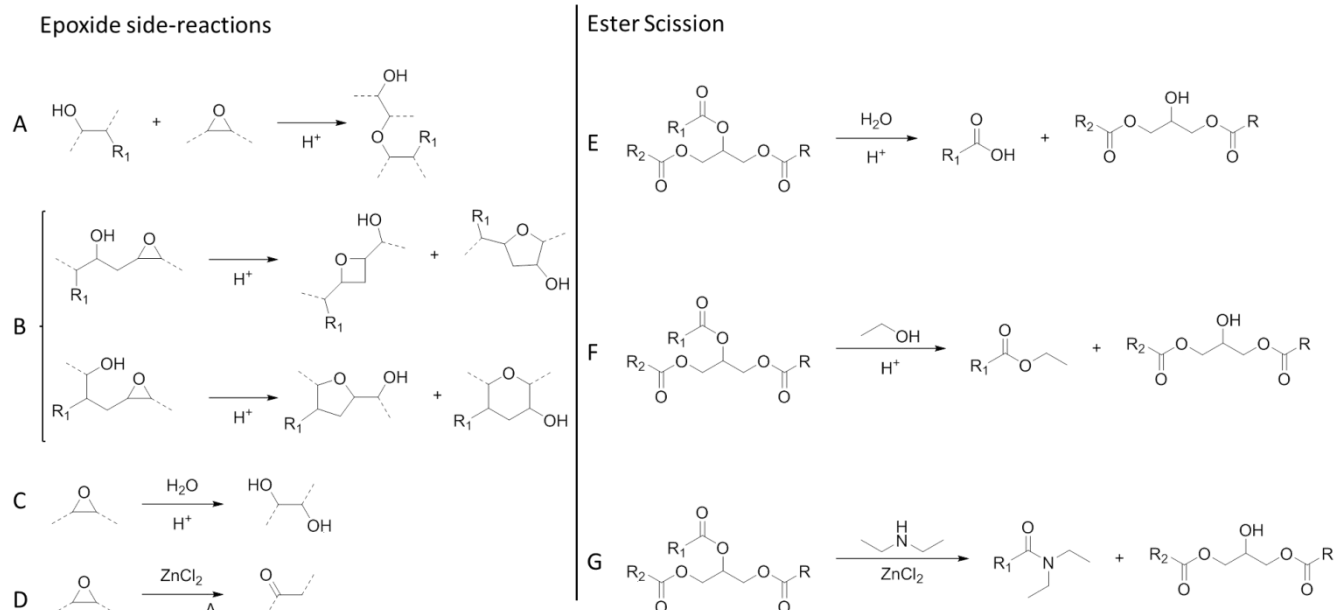
Scheme S2. Side reactions occurring during polyol synthesis.

Another side reaction that can occur under acidic conditions is linked to the epoxide ring-opening by the remaining moisture in the medium (Scheme S2-**C**).[17] However, the hydrophobic character of triglycerides reduces this side reaction.[18] Moreover, such a side reaction would increase polyols I_{OH}. On the contrary, the epoxide ring-opening using a secondary amine and catalyzed by $ZnCl_2$ can induce epoxide isomerization (Scheme S2-**D**). This side reaction was observed for temperatures superior to 100 °C and $ZnCl_2$ was used as a catalyst.[19] The presence of acid is promoting this side reaction. The side reactions on the epoxide group can explain the average conversion of epoxide to hydroxyl.
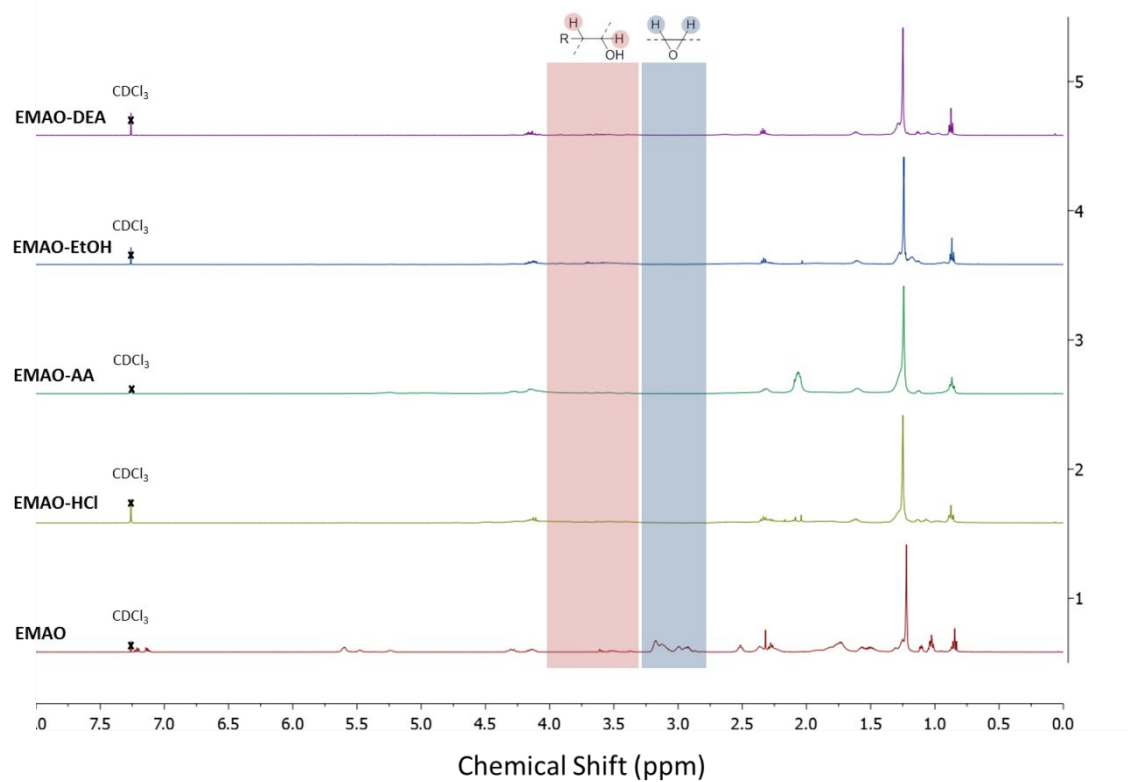
Figure S5. Stacked proton NMR spectra of polyols from EMAO.
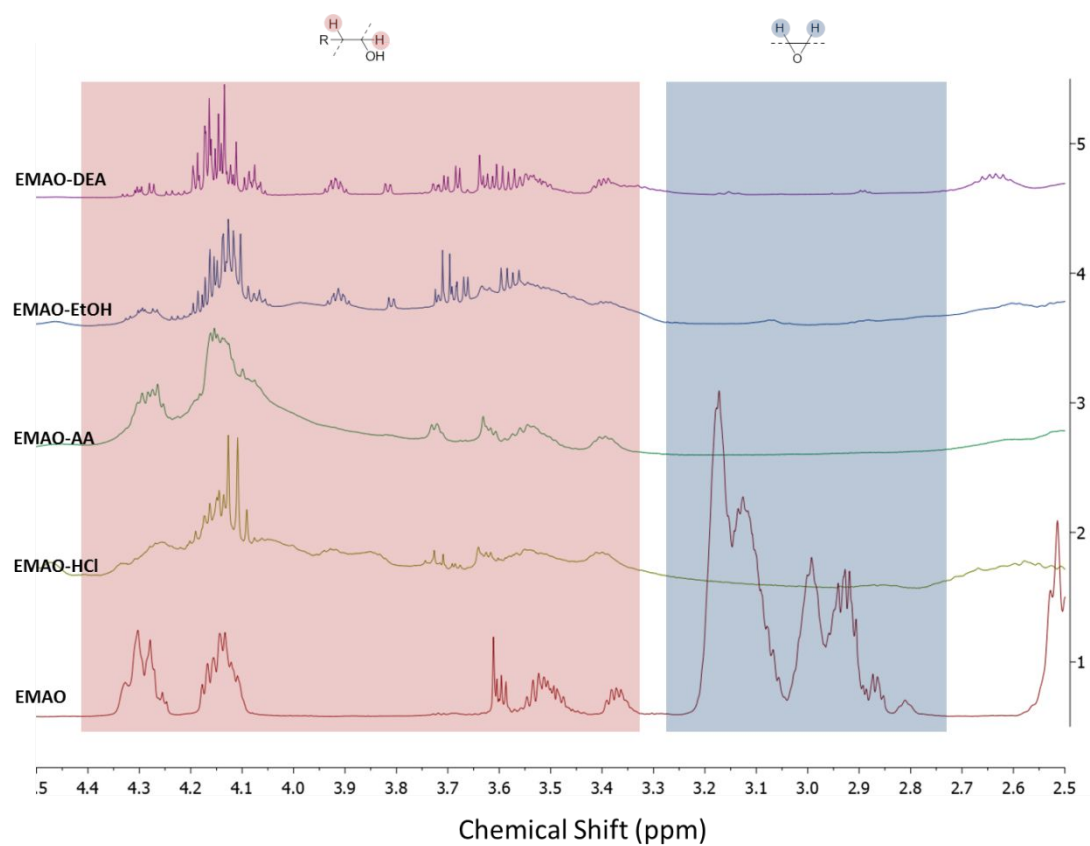
Figure S6. Stacked proton NMR spectra of polyols from EMAO (zoom from 4.5 to 2.5 ppm).

Acidity analysis

In the PU industry, polyols are notably characterized by their acidity index. The acids can slow the PU network formation by coordination and thus induce deactivation of catalysts. The the I_A of crude polyols was between 60 and 100 mg KOH/g. Basic washings were performed on the crude polyols using sodium bicarbonate ($NaHCO_3$) and should have removed most of the residual acid reagents. EMAO-AA and EMAO-HCl acidity index were 21.8 and 9.4 mg KOH/g, respectively. One reason for this high acidity can be related to the presence of fatty acid formed and residual acid reagents used for the polyols syntheses. The fatty acid formation during polyol synthesis via side reactions was confirmed by high retention times in SEC characterization. In the case of EMAO-DEA, the tertiary amine present on the polyol structure shielded the acidity. Thus the acidity index could not be performed.

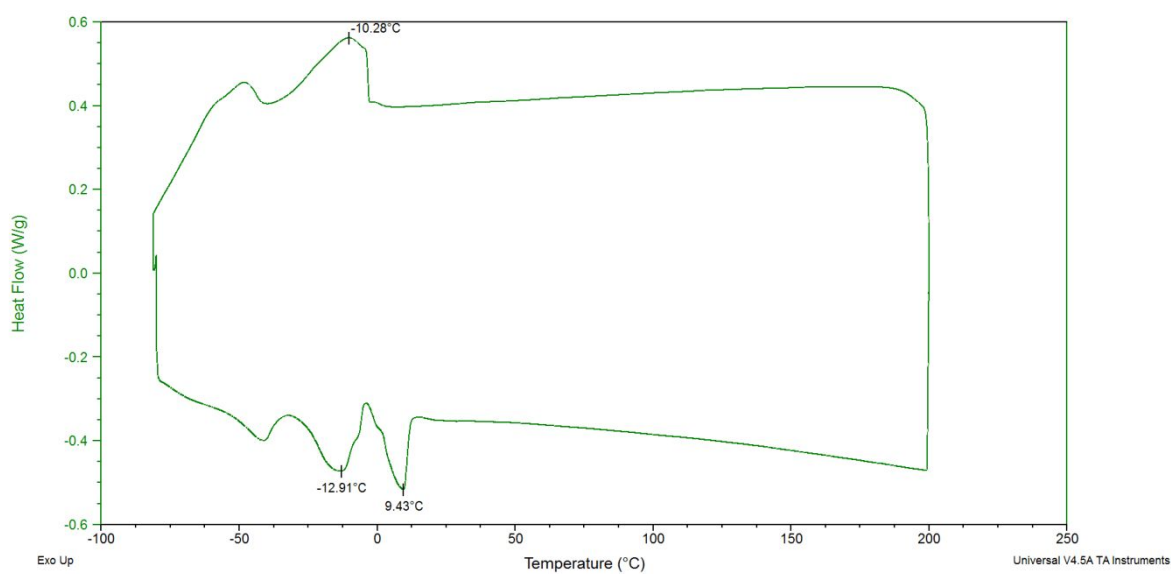Crystallization and viscosity behavior with temperature of the different polyols
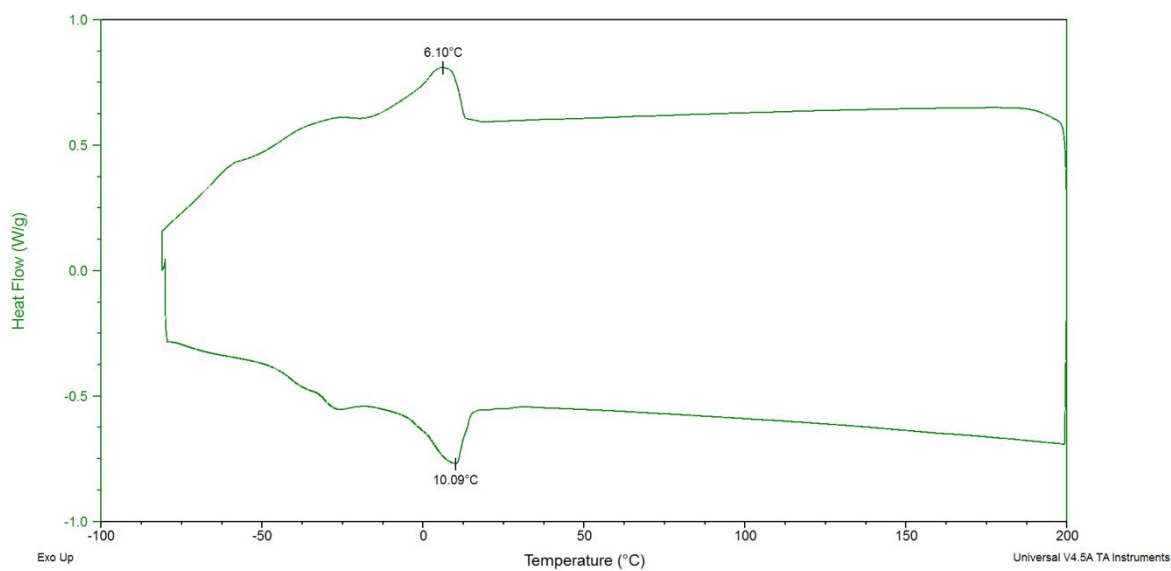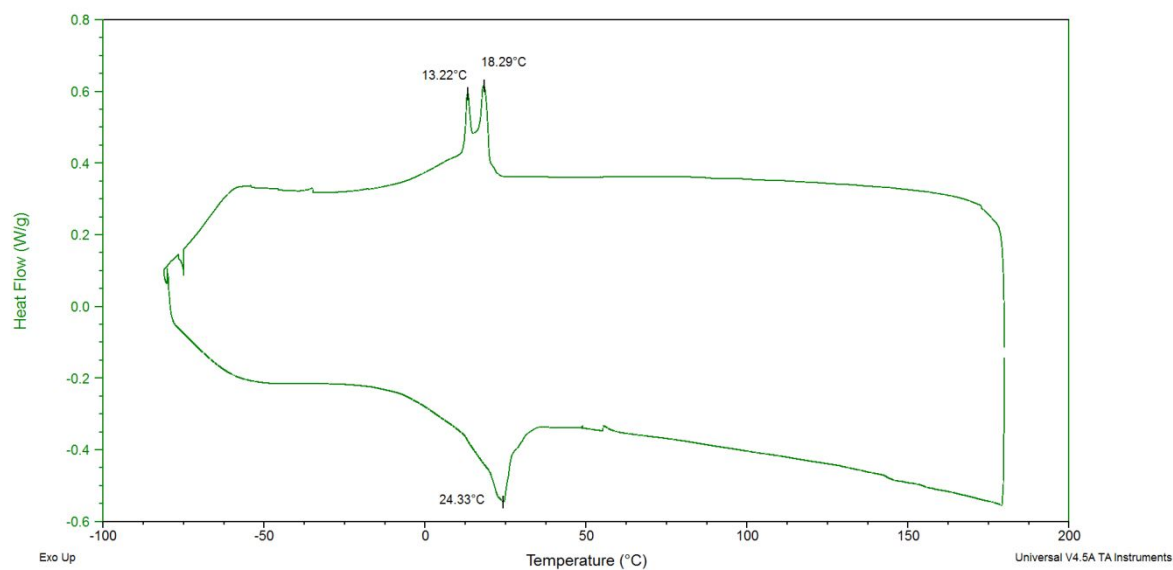

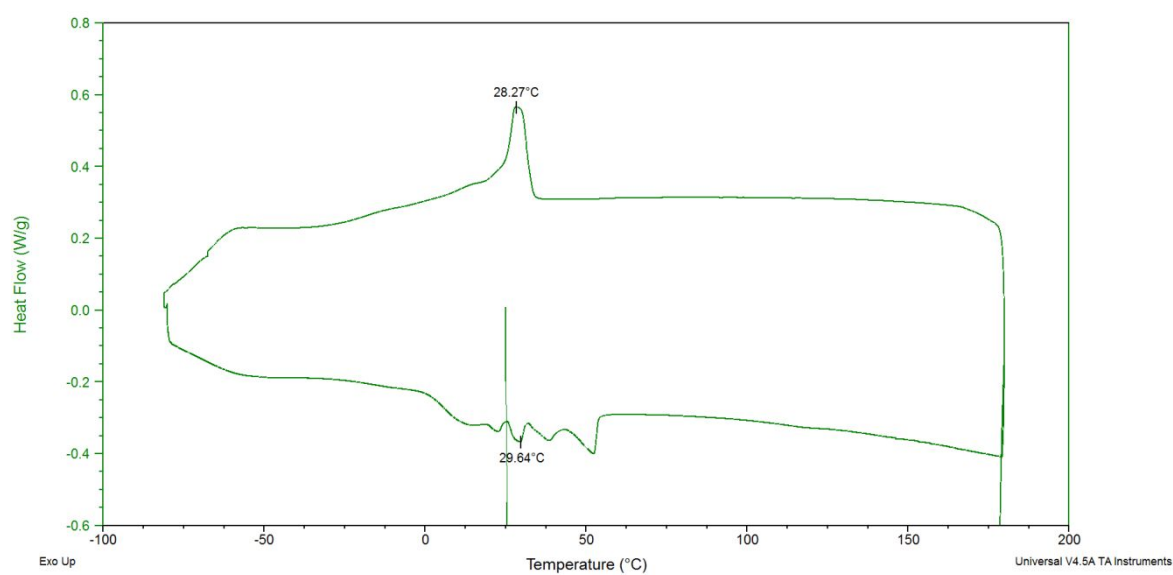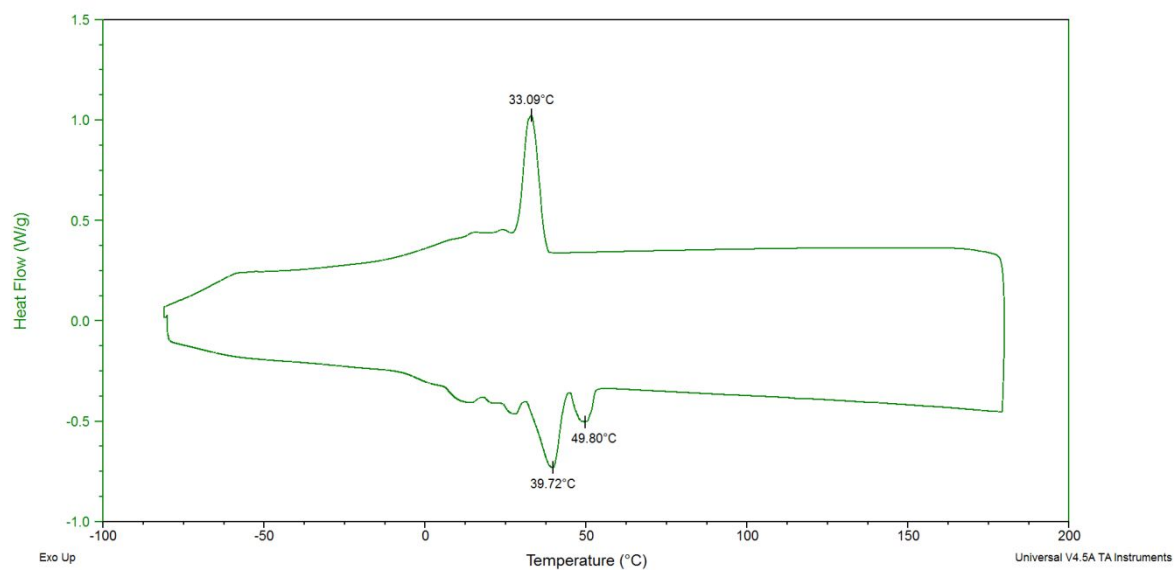**Figure S7.** DSC thermogram of MAO.

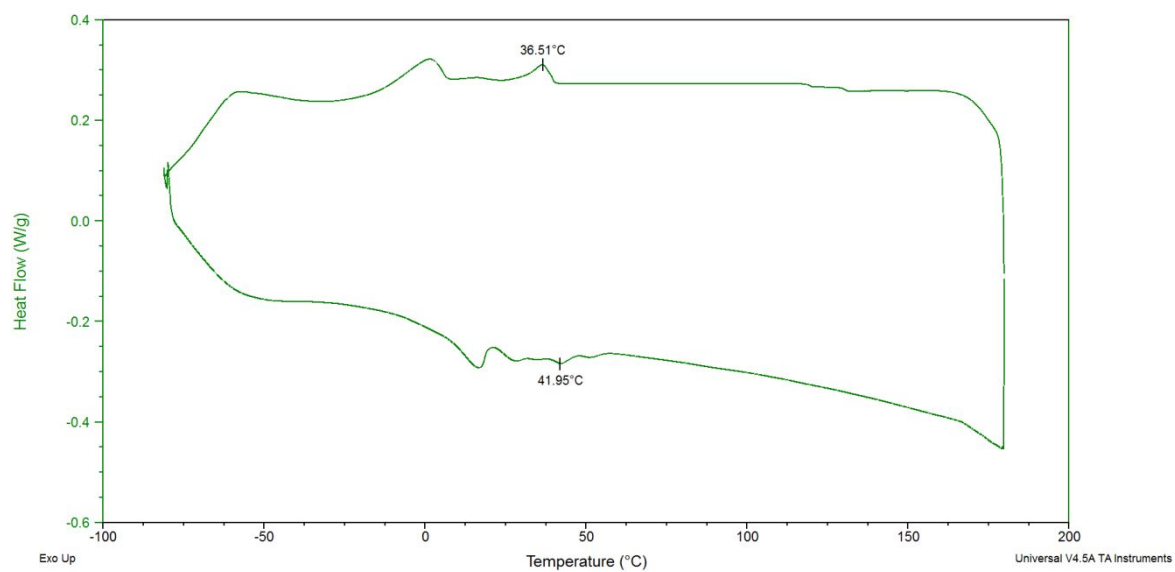**Figure S8.** DSC thermogram of EMAO.
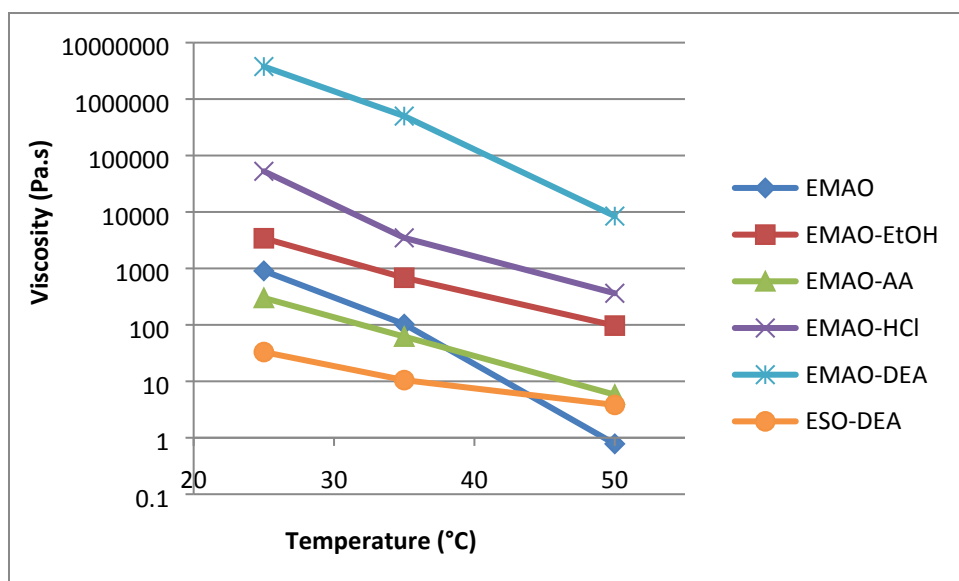
Figure S9. DSC thermogram of EMAO-AA.

Figure S10. DSC thermogram of EMAO-EtOH.

Figure S11. DSC thermogram of EMAO-DEA.

Figure S12. DSC thermogram of EMAO-HCl.

Figure S13. Evolution of the viscosity with temperature of EMAO (◆), EMAO-EtOH (■), EMAO-AA(▲), EMAO-HCl (✕), EMAO-DEA(✳) and ESO-DEA (●).

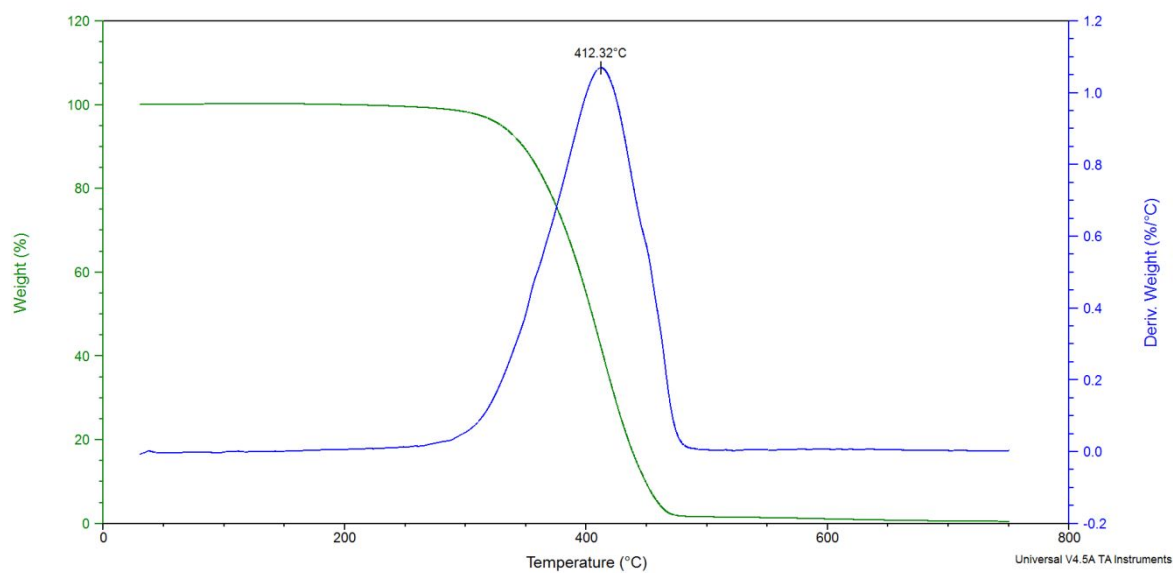Thermal stability of MAO, EMAO and polyols

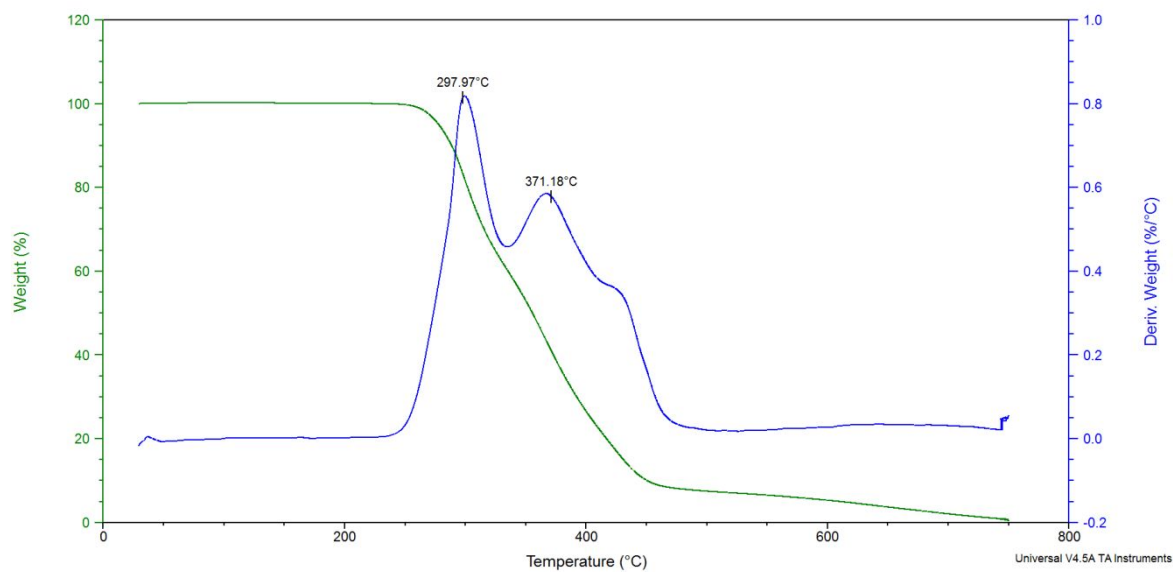**Figure S14.** TGA thermogram of MAO.

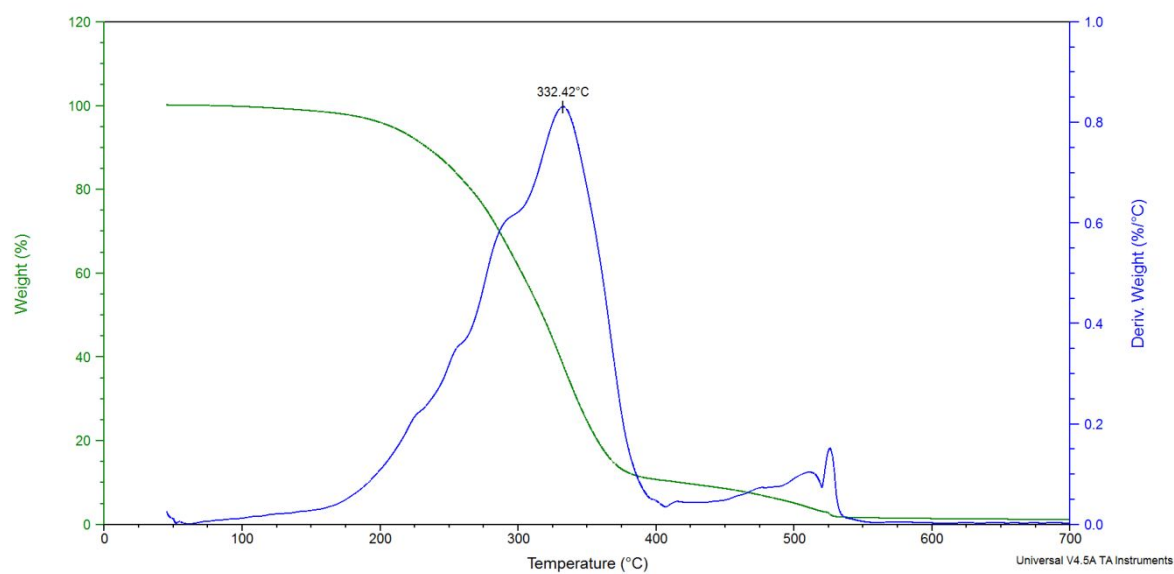**Figure S15.** TGA thermogram of EMAO.
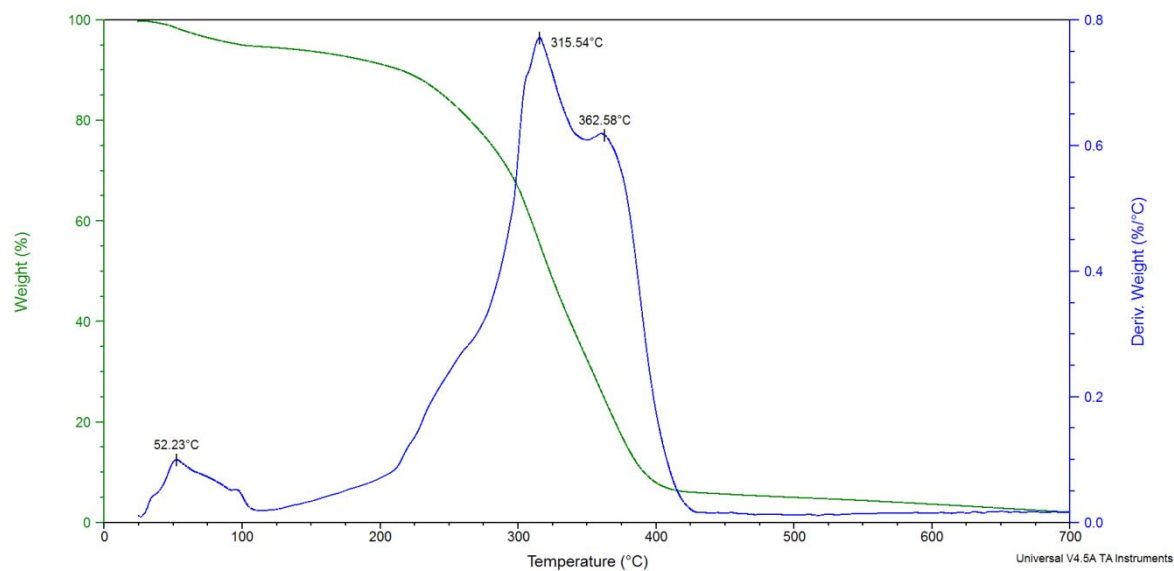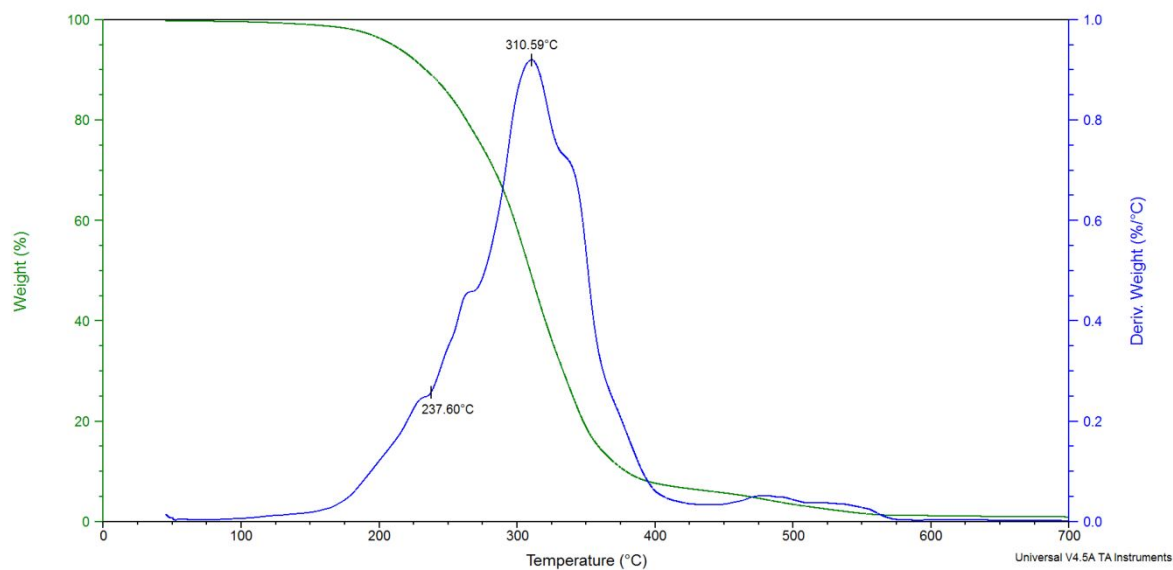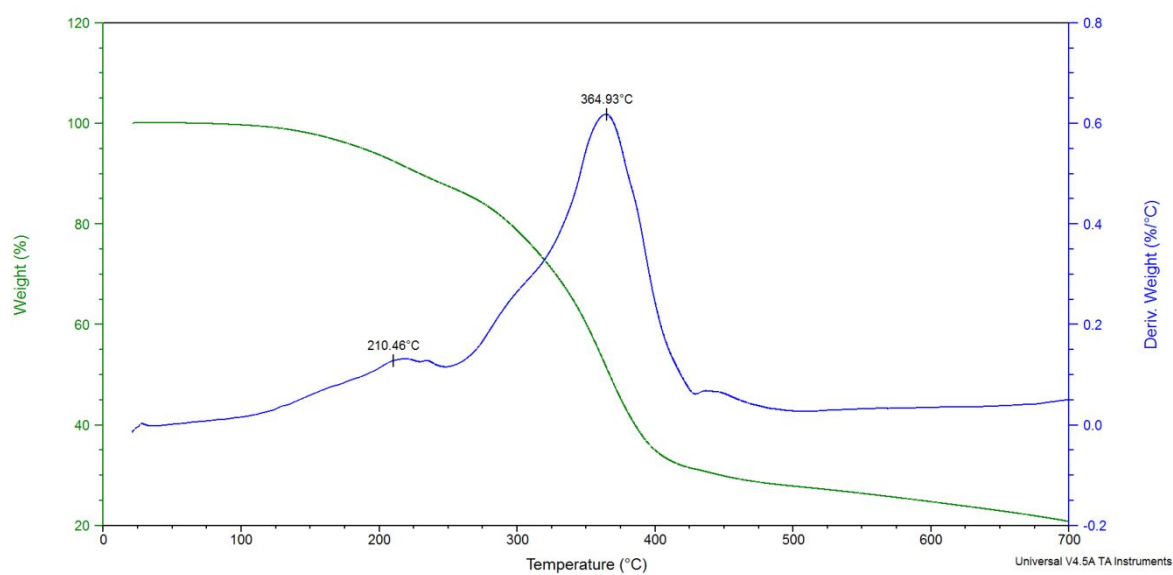
Figure S16. TGA thermogram of EMAO-AA.

Figure S17. TGA thermogram of EMAO-EtOH.

Figure S18. TGA thermogram of EMAO-DEA.

Figure S19. TGA thermogram of EMAO-HCl.

Foams characteristic times and reactivity determined by Foamat measurements

Table S3. Cream, gel and tack-free times and final height for the different foams.

	Ref	AA 25	DEA 25	HCl 25	EtOH 25	EtOH 35	EtOH 50	EtOH 75	ESO-DEAcat
Characteristic time (s)									
Cream Time	12 ± 1	21 ± 1	9 ± 1	21 ± 1	15 ± 1	17 ± 1	18 ± 1	19 ± 1	180 ± 1
Gel Time	47 ± 3	79 ± 3	35 ± 3	60 ± 3	53 ± 3	58 ± 3	67 ± 3	91 ± 3	650 ± 3
Tack-free time	62 ± 8	123 ± 8	60 ± 8	91 ± 8	84 ± 8	103 ± 8	113 ± 8	155 ± 8	1200 ± 8
Final height (cm)	18.9 ± 0.2	18.9 ± 0.2	17.4 ± 0.2	18 ± 0.2	19.1 ± 0.2	18.8 ± 0.2	18.1 ± 0.2	15.8 ± 0.2	14.5 ± 0.2

Figure S20. Expansion rate (mm/s) determined with the Foamat device for Ref (▬), EtOH35 (▬), EtOH50 (▬), EtOH75 (▬), ESO-DEAcat (▬).

Foam cells morphology
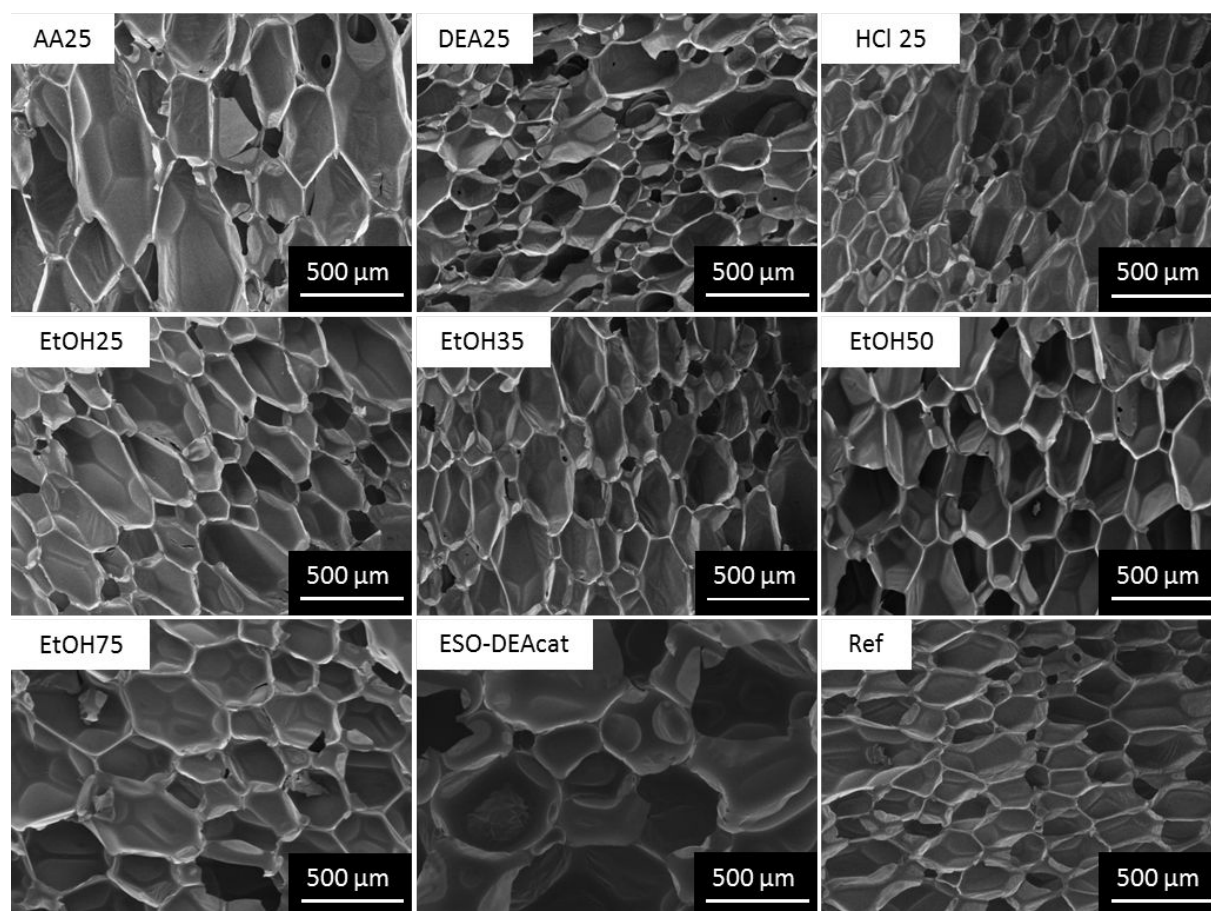
Figure S21. SEM images of all formulations in the longitudinal direction.
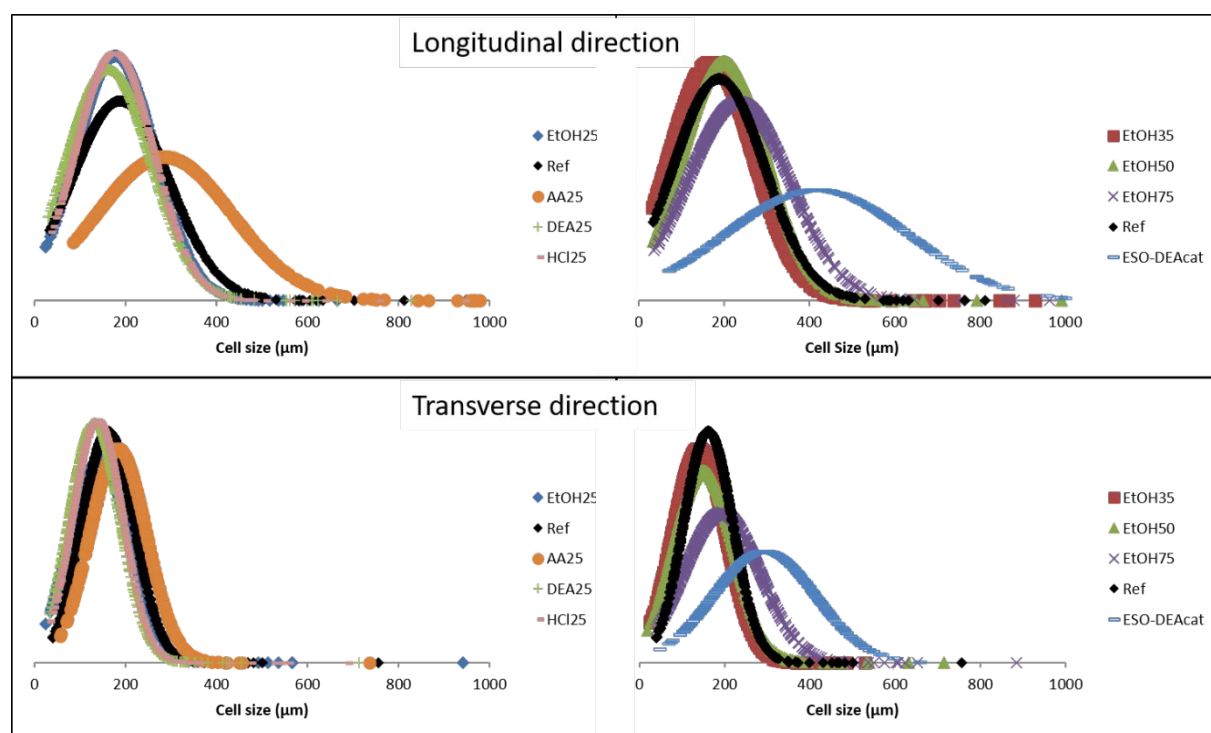
Figure S22. Representation of cell size modeled by a central binomial distribution.

Foams core-temperature during foam process determined by Foamat measurements
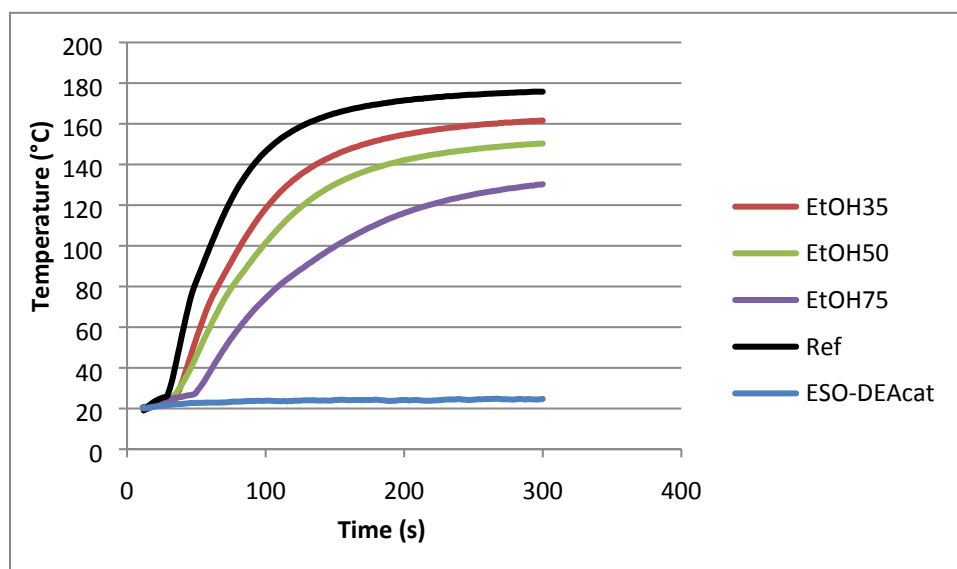
Figure S23. Temperature at the center of the foam recorded with the Foamat device of EtOH 35 (—), EtOH50 (—), EtOH75 (—), Ref (—) and ESO-DEAcat (—).
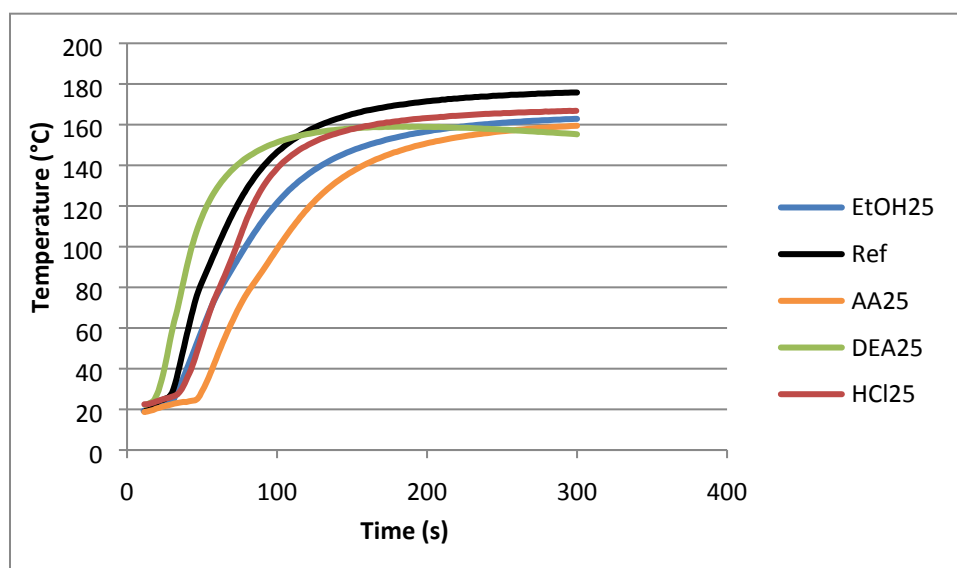
Figure S24. Temperature at the centre of the foam recorded with the Foamat device of A: EtOH25 (—), Ref (—), AA25 (—), DEA25 (—), HCl25 (—).

The density of the foams

Table S4. Density of the different foams.

	Ref	AA 25	DEA 25	HCl 25	EtOH 25	EtOH 35	EtOH 50	EtOH 75	ESO-DEAcat
Density (kg/m³)	31 ± 2	29 ± 1	30 ± 1	31 ±1	28 ± 1	28 ± 1	30 ± 1	32 ± 1	36 ± 1

Synthesis and characterization of a catalytic polyol with ESO

Ring-opening of ESO with diethylamine

The protocol was adapted from a previously published work.[10,12] The reaction was carried out in a round bottom flask equipped with a reflux condenser and a mechanical stirrer. The flask was filled with 100 g of ESO 4.1 mmol epoxide/g, (0.41 mol, 1 eq), 10 g of $ZnCl_2$ (0.07 mol, 0.18 eq) and 50 mL of diethylamine (0.48 mol, 1.2 eq). The mixture was stirred at 90 °C for 24 hours. The catalyst was removed by filtration. 100 mL of ethyl acetate were added to decrease the viscosity of the mixture. Then the organic phase was treated with $NaHCO_3$ and water until the pH was neutral. Then it was washed with brine solution, dried with anhydrous sodium sulfate and then filtered. The solvent was evaporated under reduced pressure. The ring-opened ESO with diethylamine (ESO-DEA) was dried overnight in a vacuum oven at 40 °C. The yield determined by NMR was 59 mol%.

^{1}H NMR (400 MHz, CDCl$_3$): δ= 5.25 (tt, 1H; CH-Glycerine), 4.30 (d, 2H; CH$_2$-Glycerine), 4.15 (d, 2H; CH$_2$-Glycerine), 3.2-2.8 (m, 2H; epoxide) 1.35–1.13 (m, 30H; aliphatic CH$_2$), 0.88 ppm (t, 3H; CH$_3$)
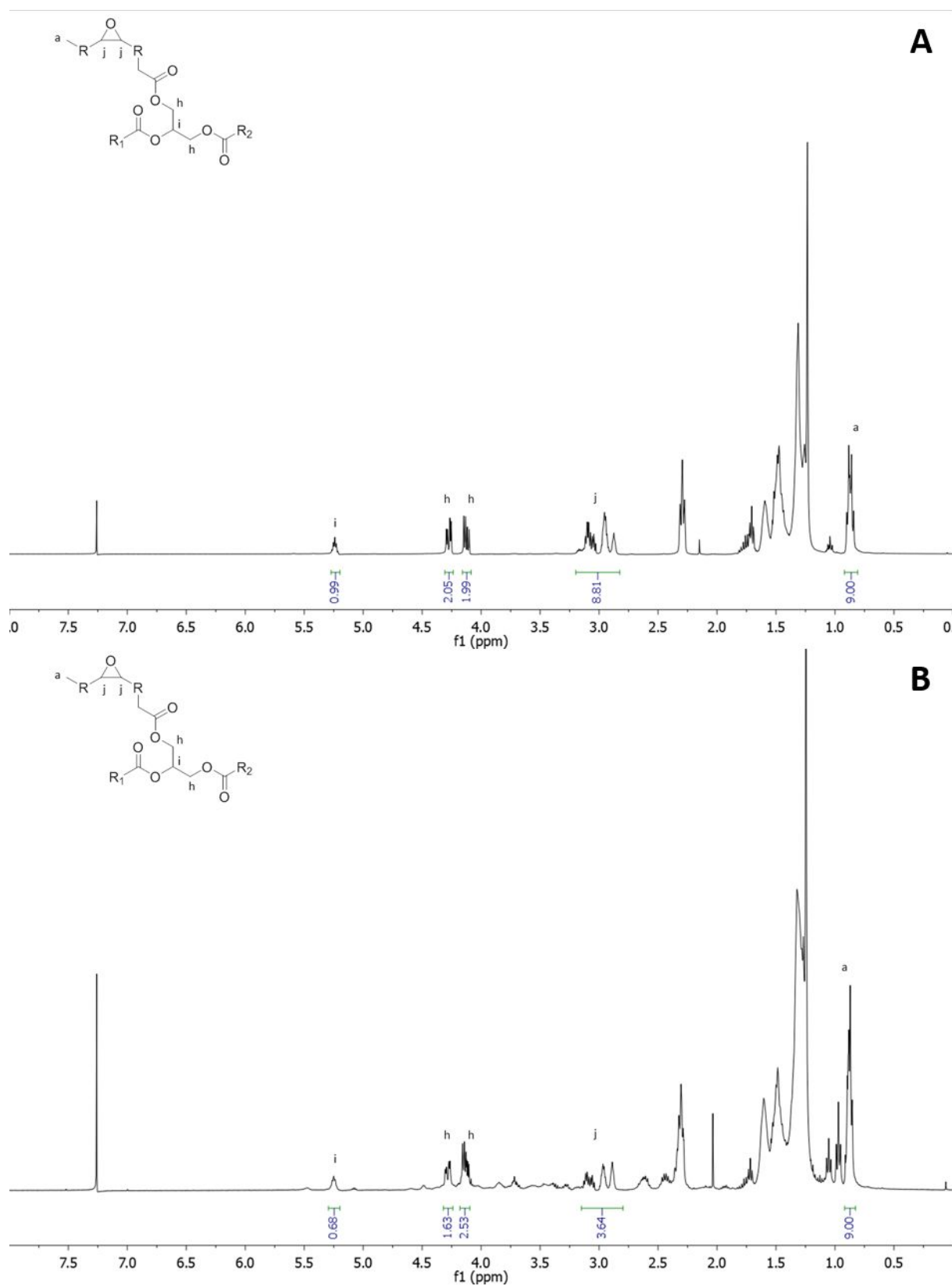
Figure S25. Proton NMR spectrum of ESO (**A**) and ESO-DEA (**B**).

Calculation of the real I_{OH} from ^{31}P I_{OH} and epoxide index

The epoxide index unit is changed from the percentage of oxygen to mol epoxide/g by Equation S7:

$$EO(mol\_epoxide/g) = \frac{EO(\%O)}{1600} \tag{S7}$$

Assuming full conversion of epoxide in hydroxyl without side-reactions, the quantity in moles of epoxide is the same as the quantity of hydroxyl, but the molar mass is changing with the addition of the ring-opening reagent. In this case, the diethylamine (73.14 g/mol) was taken as the ring-opening reagent. From the EO (mol_epoxide/g), the theoretical I_{OH} in mol OH/g can be calculated by Equation S8.

$$I_{OH_{Th}} = \frac{EO(mol\_epoxide/g)}{(1 + 73.14 * EO(mol\_epoxide/g))} \tag{S8}$$

The transformation of the IOH (mol OH/g) in mg KOH/g is done with Equation S9.

$$I_{OH}(mgKOH/g) = I_{OH}(mol\_OH/g) * 56100 \tag{S9}$$

The real I_{OH} is calculated from the I_{OH} results from 31P measurement and the epoxide index with Equation S10.

$$\mathrm{Re}al\_I_{OH}(mgKOH/g) = I_{OH}(mol\_OH/g) - EO(mol\_epoxide/g) \tag{S10}$$

Calculations were done on the partially ring-opened ESO by diethylamine and synthesized in Table S5.

Table S5. Calculation of the real IOH index results and conversions.

Characterization	Unit	Result	Conversion (function)
Initial epoxide	% OE	6.6	
index	mmol epoxide/g	4.13 ± 0.06	
Epoxide index	% OE	2.1 ± 0.1	68 % (epoxide)
	mmol epoxide/g	1.31 ± 0.06	
I_{OH} exp	(mg KOH/g)	190 ± 10	
	mmol OH/g	3.39 ± 0.2	
I_{OH} th	(mg KOH/g)	180	
Real IOH	(mg KOH/g)	120 ± 10	66 % (OH)

| mmol OH/g | 2.1 ± 0.1 |

The NMR conversion based on Figure S25 is 59 %.
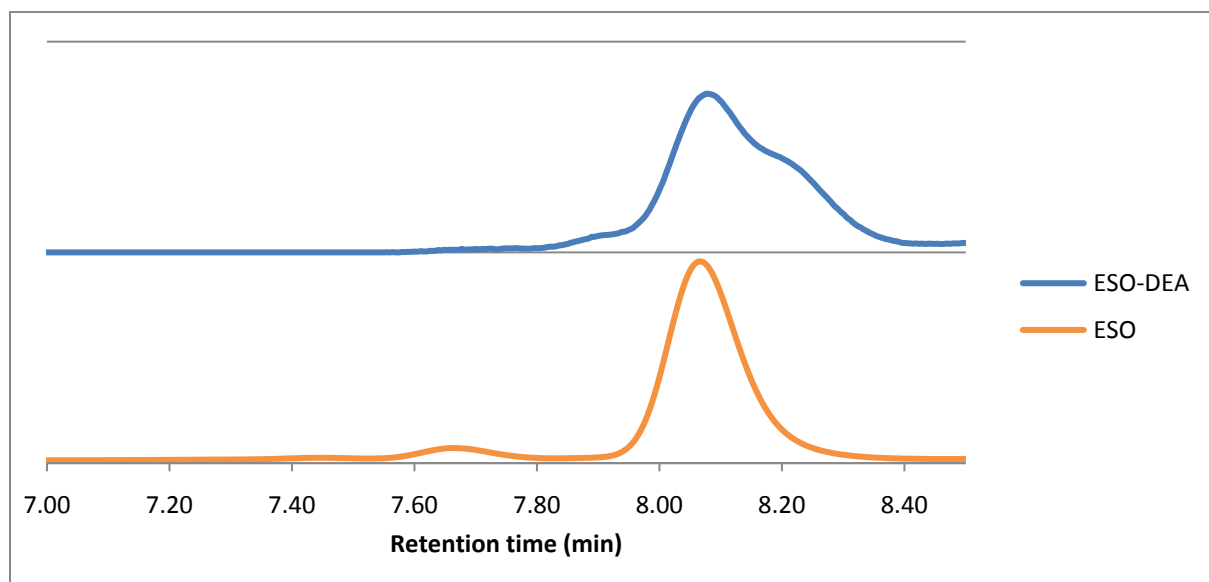
Figure S26. Size exclusion chromatography of ESO (━) and ESO-DEA (━).

Thermal conductivity theory

The thermal conductivity (λ) of the foams is related to the total heat transfer (q_t) passing

through the foam, as described by Equation S11.

$$\lambda = q_t * \frac{L}{\Delta T}$$

(S11)

Where q_t has three components described in Equation S12: the conduction through the

polymer matrix (q_{PUR}), through the gas phase (q_{gas}) and the radiation (q_{rad}). The convection

transfer is negligible for closed-cell porous materials with a cell size inferior to 3 mm.[20]

$$q_t = q_{PUR} + q_{gas} + q_{rad} + q_{conv}$$

(S12)

FTIR characterizations of foams
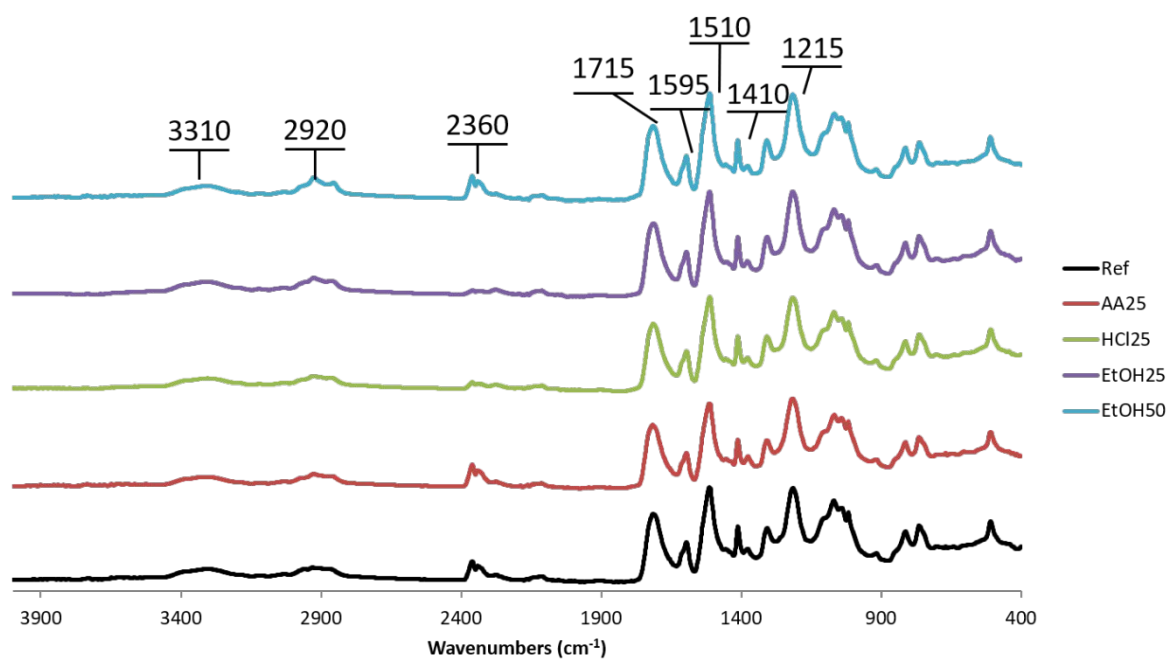
Figure S27. FTIR spectra in absorbance mode of Ref (━━), AA25 (━━), HCl25 (━━), EtOH25 (━━), EtOH50 (━━) foams.

Fire behavior of foams

Foam fire behavior was evaluated according to the EN ISO 11925-2 standard method. This flammability test consists of exposing a plane foam sample for 15 seconds to a small direct flame (20 mm high). This flammability test is evaluated by measuring the maximum flame propagation on the plane surface of the foam. The persistence of flame on samples after exposure to the direct flame was timed.

In order to reduce the flammability of the PUF,[21] flame retardants Tris(1-chloro-2propyl) phosphate (TCPP) was used in the formulations (Table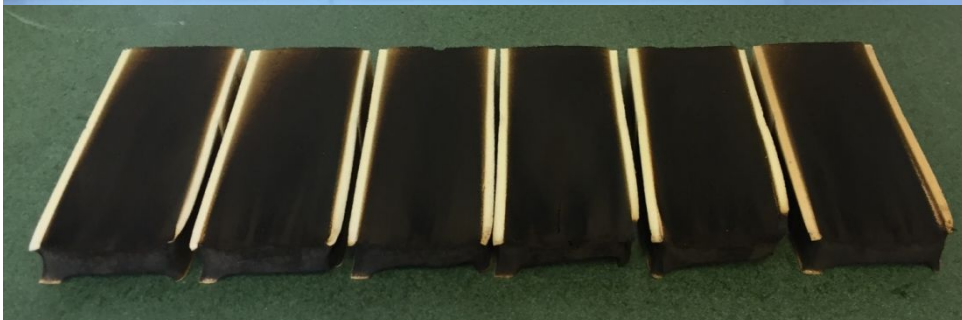 2). TCPP is a phosphorous-based compound used in the PU formulation and, in the presence of fire, creates a carbonaceous (char) barrier. The system is denoted as intumescent if the char layer is foamed by the gas released by the thermal degradation of the material.[22] This barrier protects the material from flame exposition and limits the transfer of oxygen toward the flame.[22] The intumescent behavior is heightened by the aromatic structure of the isocyanate.[21] It acts as a radical scavenger, limiting the oxidation propagation and then forms a char layer by condensation of partially oxidized aromatic species.[21] Figure S28 displays 18 cm long cross-section of the previously mentioned foams once exposed to a 2 cm long flame at the bottom of the foam. Two reference samples were performed for this test to determine the consistency of the flame persistence time. Prior to the test, the HCl25 was brown due to the dark color of the biobased polyol. Once the test performed, all samples present a carbonaceous black layer (Figure S28).

		Ref1	Ref2	EtOH25	EtOH50	AA25	HCl25
Flame Height	cm	> 18 cm	> 18 cm	> 18 cm	> 18 cm	> 18 cm	> 18 cm
Persistancy	s	26 s	21 s	22 s	38 s	30 s	24 s

Figure S28. Results of the flammability test for Ref, EtOH25, EtOH50, AA25 and HCL25 foams.

The flame height and the carbon layer on the samples indicated flame propagation throughout the entire surface of the sample. All samples burned so fast that the flame retardant only limits the flame propagation. The char layer formed did not stop the propagation of the fire and it spread along the foam. The persistence of the flame was more significant in EtOH50. Furthermore, the foam had a cracked surface after the test. The substitution of 50 % of fossil-based polyol by a biobased one decreases the intumescent character. The polyols synthesized at the lab scale could contain residual solvent, favoring fire propagation. As displayed in TGA thermogram of EMAO-EtOH Figure S17 in SI, some weight loss occurs at temperatures below 100 °C. This could correspond to some traces of ethanol or ethyl acetate. Moreover, MAO contains C16:0 fatty acids, long alkane carbonated chains that can quickly burn. As previously discussed, EMAO-HCl had higher thermal stability due to the presence of chlorine, so improved fire behavior of HCl25 was expected.[23,24] Nevertheless, HCl25 has the same

flammability results as reference materials. The result of this flammability test for HCl25 was insufficient to assess further the flame retardant activity of EMAO-HCl25.

The TGA results depicted in Figure S29 and Table S6 in SI showed a similar weight loss profile for all foams. The temperature at 5 % ($T_{5\%}$) and 50 % ($T_{50\%}$) weight loss were around 220 °C and 360 °C, respectively. The PU polymer matrix was characterized by three significant steps of degradation. The first degradation was characteristic of the hard segments, the second degradation stage was related to the rigid part of the PU network, and the last step was the degradation of the more thermally stable isocyanurate formed partially as a secondary product[25] during the foaming process and partially during the dissociation of the urethane bond.[26] The foam system is complex and composed of several different chemical groups (urethane, urea, ester, etc.) whose degradation can coincide.
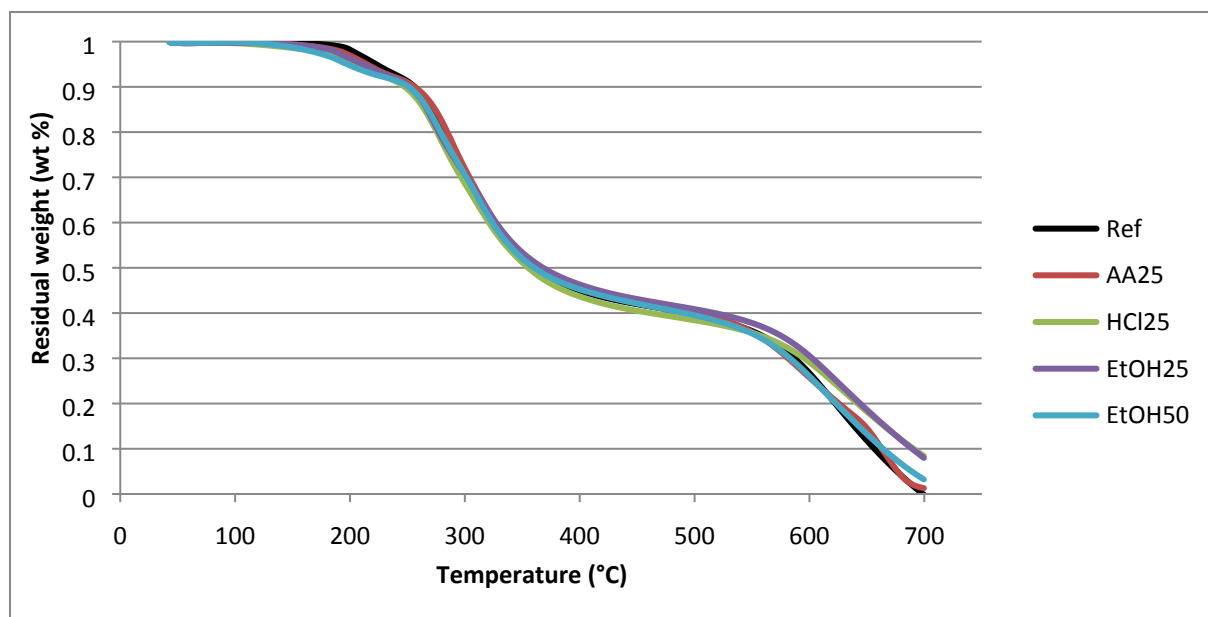
Figure S29. TGA of Ref (━), AA25 (━), HCl25 (━), EtOH25 (━) and EtOH50 (━) foam under nitrogen.

Table S6. TGA and DTG data for Ref, AA25, HCl25, EtOH25 and EtOH50 foam.

		Ref	AA25	HCl25	EtOH25	EtOH50
TGA	$T_{5\%}$	223	206	219	218	204
	$T_{50\%}$	359	358	367	361	356
	T_{deg}					
DTG	max 1	280	279	288	273	277
	T_{deg}					
	max 2	331	315	312	318	311
	T_{deg}					
	max 3	615	615	660	615	620

Bibliography

(1)   Argyropoulos, D. S.; Bolker, H. I.; Heitner, C.; Archipov, Y. [31] P NMR Spectroscopy in Wood Chemistry. Part IV. Lignin Models: Spin Lattice Relaxation Times and Solvent Effects in [31] P NMR. *Holzforschung* **1993**, *47* (1), 50–56. https://doi.org/10.1515/hfsg.1993.47.1.50.

(2)   Korntner, P.; Sumerskii, I.; Bacher, M.; Rosenau, T.; Potthast, A. Characterization of Technical Lignins by NMR Spectroscopy: Optimization of Functional Group Analysis by 31P NMR Spectroscopy. *Holzforschung* **2015**, *69* (6), 807–814. https://doi.org/10.1515/hf-2014-0281.

(3)   Dais, P.; Spyros, A. 31P NMR Spectroscopy in the Quality Control and Authentication of Extra-Virgin Olive Oil: A Review of Recent Progress. *Magn. Reson. Chem.* **2007**, *45* (5), 367–377. https://doi.org/10.1002/mrc.1985.

(4)   Flory, P. J. Molecular Size Distribution in Three Dimensional Polymers. I. Gelation [1]. *J. Am. Chem. Soc.* **1941**, *63* (11), 3083–3090. https://doi.org/10.1021/ja01856a061.

(5)   Stockmayer, W. H. Theory of Molecular Size Distribution and Gel Formation in Branched Polymers II. General Cross Linking. *The Journal of Chemical Physics* **1944**, *12* (4), 125–131. https://doi.org/10.1063/1.1723922.

(6)   Winter, H. H.; Chambon, F. Analysis of Linear Viscoelasticity of a Crosslinking Polymer at the Gel Point. *Journal of Rheology* **1986**, *30* (2), 367–382. https://doi.org/10.1122/1.549853.

(7)   Chambon, F.; Winter, H. H. Linear Viscoelasticity at the Gel Point of a Crosslinking PDMS with Imbalanced Stoichiometry. *Journal of Rheology* **1987**, *31* (8), 683–697. https://doi.org/10.1122/1.549955.

(8)   Andersons, J.; Kirpluks, M.; Stiebra, L.; Cabulis, U. Anisotropy of the Stiffness and Strength of Rigid Low-Density Closed-Cell Polyisocyanurate Foams. *Materials & Design* **2016**, *92*, 836–845. https://doi.org/10.1016/j.matdes.2015.12.122.

(9)   Arbenz, A.; Perrin, R.; Avérous, L. Elaboration and Properties of Innovative Biobased PUIR Foams from Microalgae. *J Polym Environ* **2018**, *26* (1), 254–262. https://doi.org/10.1007/s10924-017-0948-y.

(10)   Peyrton, J.; Chambaretaud, C.; Avérous, L. New Insight on the Study of the Kinetic of Biobased Polyurethanes Synthesis Based on Oleo-Chemistry. *Molecules* **2019**, *24* (23), 4332. https://doi.org/10.3390/molecules24234332.

(11)   Palaskar, D. V.; Boyer, A.; Cloutet, E.; Le Meins, J.-F.; Gadenne, B.; Alfos, C.; Farcet, C.; Cramail, H. Original Diols from Sunflower and Ricin Oils: Synthesis, Characterization, and Use as Polyurethane Building Blocks. *J. Polym. Sci. A Polym. Chem.* **2012**, *50* (9), 1766–1782. https://doi.org/10.1002/pola.25944.

(12)   Harry-O'kuru, R. E.; Tisserat, B.; Gordon, S. H.; Gravett, A. Osage Orange (*Maclura Pomifera* L.) Seed Oil Poly(α-Hydroxydibutylamine) Triglycerides: Synthesis and Characterization. *J. Agric. Food Chem.* **2015**, *63* (29), 6588–6595. https://doi.org/10.1021/acs.jafc.5b01625.

(13)   Guo, A.; Cho, Y.; Petrovic, Z. S. Structure and Properties of Halogenated and Nonhalogenated Soy-Based Polyols. 11.

(14)   Lligadas, G.; Ronda, J. C.; Galià, M.; Biermann, U.; Metzger, J. O. Synthesis and Characterization of Polyurethanes from Epoxidized Methyl Oleate Based Polyether Polyols as Renewable Resources. *J. Polym. Sci. Part A: Polym. Chem.* **2006**, *44* (1), 634–645. https://doi.org/10.1002/pola.21201.

(15)   Del Rio, E.; Galià, M.; Cádiz, V.; Lligadas, G.; Ronda, J. C. Polymerization of Epoxidized Vegetable Oil Derivatives: Ionic-Coordinative Polymerization of Methylepoxyoleate. *J. Polym. Sci. A Polym. Chem.* **2010**, *48* (22), 4995–5008. https://doi.org/10.1002/pola.24297.

(16)   Miao, S.; Zhang, S.; Su, Z.; Wang, P. Chemoenzymatic Synthesis of Oleic Acid-Based Polyesters for Use as Highly Stable Biomaterials. *J. Polym. Sci. A Polym. Chem.* **2008**, *46* (12), 4243–4248. https://doi.org/10.1002/pola.22721.

(17)   Sharma, B. K.; Adhvaryu, A.; Liu, Z.; Erhan, S. Z. Chemical Modification of Vegetable Oils for Lubricant Applications. *J Amer Oil Chem Soc* **2006**, *83* (2), 129–136. https://doi.org/10.1007/s11746-006-1185-z.

(18)   Caillol, S.; Desroches, M.; Boutevin, G.; Loubat, C.; Auvergne, R.; Boutevin, B. Synthesis of New Polyester Polyols from Epoxidized Vegetable Oils and Biobased Acids. *Eur. J. Lipid Sci. Technol.* **2012**, *114* (12), 1447–1459. https://doi.org/10.1002/ejlt.201200199.

(19)   Katritzky, A. R.; Lagowski, J. M. Heterocyclic Compounds with Three- and Four-Membered Rings. In *The Principles of Heterocyclic Chemistry*; Elsevier, 1967; pp 159–164. https://doi.org/10.1016/B978-1-4832-3304-8.50009-9.

(20)   Kuhn, J.; Ebert, H.-P.; Arduini-Schuster, M. C.; Büttner, D.; Fricke, J. Thermal Transport in Polystyrene and Polyurethane Foam Insulations. *International Journal of Heat and Mass Transfer* **1992**, *35* (7), 1795–1801. https://doi.org/10.1016/0017-9310(92)90150-Q.

(21)   Duquesne, S.; Le Bras, M.; Bourbigot, S.; Delobel, R.; Camino, G.; Eling, B.; Lindsay, C.; Roels, T.; Vezin, H. Mechanism of Fire Retardancy of Polyurethanes Using Ammonium Polyphosphate. *J. Appl. Polym. Sci.* **2001**, *82* (13), 3262–3274. https://doi.org/10.1002/app.2185.

(22)   Duquesne, S.; Le Bras, M.; Bourbigot, S.; Delobel, R.; Poutch, F.; Camino, G.; Eling, B.; Lindsay, C.; Roels, T. Analysis of Fire Gases Released from Polyurethane and Fire-Retarded Polyurethane Coatings. *Journal of Fire Sciences* **2000**, *18* (6), 456–482. https://doi.org/10.1106/6CRG-Q8VD-PV3G-ELDD.

(23)   Weil, E. D.; Levchik, S. V. Commercial Flame Retardancy of Polyurethanes. *Journal of Fire Sciences* **2004**, *22* (3), 183–210. https://doi.org/10.1177/0734904104040259.

(24)   *Fire Retardancy of Polymeric Materials*, 2nd ed.; Wilkie, C. A., Morgan, A. B., Eds.; CRC Press: Boca Raton, 2010.

(25)   Williams, R. J. J.; Vázquez, A.; Pascault, J. P. Gelation in the Cyclotrimerization of Dicyanates Considering Substitution Effects. *Polymer Bulletin* **1992**, *28* (2), 219–225. https://doi.org/10.1007/BF00299659.

(26)   Chattopadhyay, D. K.; Webster, D. C. Thermal Stability and Flame Retardancy of Polyurethanes. *Progress in Polymer Science* **2009**, *34* (10), 1068–1133. https://doi.org/10.1016/j.progpolymsci.2009.06.002.